Shallow water equations with variable topography in the resonance regime

Philippe G. LeFloch and Mai Duc Thanh

Philippe G. LeFloch
Laboratoire Jacques-Louis Lions & Centre National de la Recherche Scientifique,
Université Pierre et Marie Curie (Paris 6), 4 Place Jussieu, 75252 Paris, France.
E-mail address: lefloch@ann.jussieu.fr

Mai Duc Thanh
Department of Mathematics, International University, Quarter 6, Linh Trung Ward,
Thu Duc District, Ho Chi Minh City, Vietnam. E-mail address: mdthanh@hcmiu.edu.vn

---

Abstract

Based on an earlier work by the authors, we investigate the Riemann problem for the shallow water equations with variable topography, and we provide here for the first time a complete description of the Riemann solution, existence, uniqueness, and the case of multiple solutions of the Riemann problem are investigated. Computing strategy and algorithms for Riemann solutions are presented. Using these computing solutions of local Riemann problem, we build the Godunov scheme which turns our to be well-balanced and of quasi-conservative form. We also provide numerical tests for the Godunov scheme. In strictly hyperbolic domains, tests show that the scheme provides the convergence to the exact solution. In resonance regions, tests also provide the convergence, except that when the Godunov scheme takes its parameter states on the resonance surfaces.

Keywords: Shallow water equations, conservation law, source, Riemann problem, Godunov scheme.

---

1. Introduction

In this paper we aim at building the Godunov scheme for the initial-value problem of the following one-dimensional shallow water equations with

variable topography

$$\partial_t h + \partial_x(hu) = 0,$$
$$\partial_t(hu) + \partial_x(h(u^2 + g\frac{h}{2})) = -gh\partial_x a, \tag{1}$$

where h is the height of the water from the bottom to the surface, u is the velocity, g is the gravity constant, and $a = a(x), x \in \mathbf{R}$, is the height of the bottom from a given level. Often, the system with source (1) is supplemented with the trivial equation (as first proposed in LeFloch (1989))

$$\partial_t a = 0, \tag{2}$$

so that the new system is hyperbolic and in nonconservative form and can be handled within the Dal Maso-LeFloch-Murat theory by Dal Maso, LeFloch, and Murat (1995), Hou and LeFloch (1994), LeFloch (1988), LeFloch and Liu (1993). Since the Godunov scheme involves the solving of local Riemann problems, Riemann solutions of (1)-(2) should be constructed in such a way that they are reliable for computing purposes. Recall that the Riemann problem for (1)-(2) is the Cauchy problem with initial data (Riemann data) of the form

$$(h, u, a)(x, 0) = \begin{cases} (h_L, u_L, a_L), & x < 0, \\ (h_R, u_R, a_R), & x > 0. \end{cases} \tag{3}$$

We therefore review the Riemann problem for (1)-(2), provide the explicit constructions of solutions, observe the existence for large domain of initial data and the uniqueness. Moreover, we also describe the case of multiple solutions, giving necessary and sufficient conditions for the existence of three distinct solutions.

In our previous work LeFloch and Thanh (2007), the Riemann problem for (1)-(2) is investigated, where constructions of Riemann solutions were given. The results in our earlier work LeFloch and Thanh (2007) is improved in this paper where we present a complete description of the Riemann solution: existence, uniqueness, and the case of multiple solutions of the Riemann problem are carefully investigated. Besides, in a recent work Chinnayya, LeRoux, and Seguin (2004) the authors also addressed the Godunov method for system (1)-(2) where the exact Riemann solvers are given using their method of "continuation": starting the construction as if the bottom is flat, they try to make the construction for non-flat bottom emerge. And they construct Riemann solutions using this method in the region where the nonlinear characteristic fields are separated by the linearly degenerate one

corresponding to the eigenvalue identically zero. In this region, the solution with non-flat bottom still follows the two wave curves in the nonlinear characteristic fields with an early jump by a stationary wave before reaching the intersection point of these two curves. The number of waves in a Riemann solution is not bigger than the number of characteristic fields. This gives a geometrical explanation for the method. However, for Riemann data in the other two strictly hyperbolic regions, or of "cross-region" type, we find it hard to apply this method. There is always a major difference between the "flat-bottom" and "non-flat-bottom" cases, since one case the system is strictly hyperbolic, the other case the system is not strictly hyperbolic. In the non-flat-bottom case new wave curves appear taking the role of the standard wave curves. In other words, there are new wave curves on which the solution strictly follows. The number of waves in a Riemann solution can eventually be bigger than the number of characteristic fields as waves in the same family can be repeated. The appearance of such new wave curves cannot be justified from a continuation process. Thus, our goal is to present computing algorithms for Riemann solutions given by explicit constructions, and then use these computing solutions of local Riemann problems to build the Godunov scheme. We also provide numerical tests. In strictly hyperbolic domains, tests show that the scheme provides the convergence to the exact solution. In resonance regions, tests also provide the convergence, except that when the Godunov scheme takes its parameter states on the resonance surfaces.

As well-known, the system (1) is not strictly hyperbolic as characteristic fields may coincide on certain surfaces. The study of non-strictly hyperbolic systems has been attracted many authors. See LeFloch (1989), Marchesin and Paes-Leme (1986), LeFloch and Thanh (2003), Thanh (2009) for the model of fluid flows in a nozzle with variable cross-section, Isaacson and Temple (1995, 1992), GoatinLeFloch (2004), Andrianov and Warnecke (2004,?) for other models.

It is interesting that the Godunov scheme for (1)-(2) is well-balanced: it captures exactly stationary waves. We observe that well-balanced scheme for shallow water equations have been considered by many authors, see Greenberg and Leroux (1996), Thanh, Fazlul K., and Ismail (2008), Jin and Wen (2004, 2005), Gallouët, Hérard, and Seguin (2004). The work of discretization of nonconservative system of balance laws or systems with source terms also attracts many authors, see for example Greenberg et al (1997), Botchorishvili, Perthame and Vasseur (2003), Botchorishvili and Pironneau

(2003), Gosse (2000), Audusse et al (2004) for a single conservation law with source. Well-balanced schemes were presented in Kröner and Thanh (2005), Kröner, LeFloch, and Thanh (2008), Jin and Wen (2004, 2005) for the model of fluid flows in a nozzle with variable cross-section. Well-balanced schemes for multi-phase flows and other models were studied in Bouchut (2004), Lallemand and Saurel (2000), Saurel and Abgrall (1999), Ambroso et al (2009), Thanh and Ismail (2009), etc. See also and the references therein.

The organization of this paper is as follows. In Section 2 we will recall basic facts of the system (1)-(2) and provide the computing method for stationary contact waves. In Section 3 the Riemann problem is revisited, where we present a new way of constructing solutions by "gluing" together different type of solution structures. Due to this, we can observe the existence of solutions for a larger domain of initial data. In Section 4 we present computing strategy for the exact Riemann solvers and then we build the Godunov scheme. Section 5 is devoted to numerical tests for the Godunov scheme using our computing exact Riemann solvers, where data belong to strictly hyperbolic domains. Here we provide test cases with different Riemann solutions. We measure the errors and observe that the errors get smaller and smaller when the mesh sizes get smaller and smaller. Section 6 is devoted to numerical tests for the Godunov scheme, where data belong to resonance regions. We observe the cases the tests give convergence and the case the test gives unsatisfactory results.

2. Shallow water equations

2.1. Wave curves

As seen by LeFloch and Thanh (2007), if we choose the dependent variable $(h, u, a) = (h, u, a)(x, t)$, the Jacobian matrix of the system admit three real eigenvalues:

$$\lambda_1(U) := u - \sqrt{gh} < \lambda_2(U) := u + \sqrt{gh}, \quad \lambda_3(U) := 0, \tag{4}$$

together with the corresponding eigenvectors:

$$r_1(U) := \left(h - \sqrt{gh} 0 \right), \quad r_2(U) := \left(h \sqrt{gh} 0 \right), \quad r_3(U) := \left(g h - g u u^2 - gh \right), \tag{5}$$

4

so that the system (1)-(2) is hyperbolic, but not strictly hyperbolic. More precisely, the first and the third characteristic fields may coincide:

$$(\lambda_1(U), r_1(U)) = (l_3(U), r_3(U))$$

on the surface

$$\mathcal{C}_+ := \{(h, u, a) | \quad u = \sqrt{gh}\} \tag{6}$$

of the phase domain. And, the second and the third characteristic fields may coincide:

$$(\lambda_2(U), r_2(U)) = (l_3(U), r_3(U))$$

on the surface

$$\mathcal{C}_- := \{(h, u, a) | \quad u = -\sqrt{gh}\} \tag{7}$$

of the phase domain. The surfaces $\mathcal{C}_\pm$, in the following referred to as the *resonance surfaces*, separate the phase domain in the (h, u, a)-space into three sub-domains in which the system is strictly hyperbolic:

$$\begin{aligned}
G_1 &:= \{(h, u, a) \in \mathbf{R}_+ \times \mathbf{R} \times \mathbf{R}_+ | \quad \lambda_1(U) > \lambda_3(U)\}, \\
G_2 &:= \{(h, u, a) \in \mathbf{R}_+ \times \mathbf{R} \times \mathbf{R}_+ | \quad \lambda_2(U) > \lambda_3(U) > \lambda_1(U)\}, \tag{8} \\
G_3 &:= \{(h, u, a) \in \mathbf{R}_+ \times \mathbf{R} \times \mathbf{R}_+ | \quad \lambda_3(U) > \lambda_2(U)\}.
\end{aligned}$$

It is convenient to set

$$\mathcal{C} := \mathcal{C}_+ \cup \mathcal{C}_-, \quad G_2^+ := \{(h, u, a) \in G_2, u \geq 0\}, \quad G_2^- := \{(h, u, a) \in G_2, u \leq 0\}.$$

Obviously, the first and the second characteristic fields (λ_1, r_1), (λ_2, r_2) are genuinely nonlinear in the phase domain, while the third characteristic field (λ_3, r_3) is linearly degenerate.

As discussed in LeFloch and Thanh (2007), across a discontinuity there are two possibilities

   (i) either the bottom height a remains constant,

   (ii) or the discontinuity is stationary (it propagates with zero speed).

In the first the case (i), the system (1)-(2) becomes the usual shallow water equations with flat bottom. We can determine the i-shock curve $\mathcal{S}_i(U_0)$ starting from a left-hand state U_0 consisting of all right-hand states U that

5

can be connected to U_0 by a Lax shock associated with the first characteristic field is given by

$$\mathcal{S}_i(U_0): \quad \Psi_i(U;U_0) := u - u_0 \pm \sqrt{\frac{g}{2}}(h - h_0)\sqrt{\left(\frac{1}{h} + \frac{1}{h_0}\right)} = 0, \quad i = 1, 2, \quad (9)$$

where $U = (h, u)$, $h > h_0$ for $i = 1$ and $h < h_0$ for $i = 2$. We also define the backward i-shock curve $\mathcal{S}_i^B(U_0)$ starting from a right-hand state U_0 consisting of all left-hand states U that can be connected to U_0 by a Lax shock associated with the first characteristic field is given by

$$\mathcal{S}_i^B(U_0): \quad \Phi_i(U;U_0) := u - u_0 \pm \sqrt{\frac{g}{2}}(h - h_0)\sqrt{\left(\frac{1}{h} + \frac{1}{h_0}\right)} = 0, \quad i = 1, 2,$$
$$(10)$$

where $U = (h, u)$, $h < h_0$ for $i = 1$ and $h > h_0$ for $i = 2$.

Is has also been seen that the bottom height a remains constant through rarefaction fans. The forward rarefaction curve $\mathcal{R}_i(U_0)$ starting from a given left-hand state U_0 consisting of all the right-hand states U that can be connected to U_0 by a rarefaction wave associate with the first characteristic field as

$$\mathcal{R}_i(U_0): \quad \Psi_i(U;U_0) = u - u_0 \pm 2\sqrt{g}(\sqrt{h} - \sqrt{h_0}) = 0, \quad i = 1, 2, \quad (11)$$

where $U = (h, u), h \leq h_0$ for $i = 1$ and $h \geq h_0$ for $i = 2$. Given a right-hand state U_0, the backward i-rarefaction curve $\mathcal{R}_i^B(U_0)$ consisting of all left-hand states U that can be connected to U_0 by a rarefaction wave associate with the first characteristic field is given by

$$\mathcal{R}_i^B(U_0): \quad \Phi_i(U;U_0) = u - u_0 \pm 2\sqrt{g}(\sqrt{h} - \sqrt{h_0}) = 0, \quad i = 1, 2, \quad (12)$$

where $U = (h, u), h \geq h_0$ for $i = 1$ and $h \leq h_0$ for $i = 2$.

Define the forward and backward wave curves in the (h, u)-plane

$$\begin{aligned} \mathcal{W}_i(U_0) &:= \mathcal{S}_i(U_0) \cup \mathcal{R}_i(U_0) = \{U \mid \Psi_i(U;U_0) = 0\}, \\ \mathcal{W}_i^B(U_0) &:= \mathcal{S}_i^B(U_0) \cup \mathcal{R}_i^B(U_0) = \{U \mid \Phi_i(U;U_0) = 0\}, \quad i = 1, 2. \end{aligned} \quad (13)$$

Besides, it has been seen in LeFloch and Thanh (2007) that the wave curves $\mathcal{W}_1(U_0), \mathcal{W}_1^B(U_0)$ being parameterized as $h \mapsto u = u(h), h > 0$, are strictly convex and strictly decreasing functions. The wave curve $\mathcal{W}_2(U_0), \mathcal{W}_2^B(U_0)$ being parameterized as $h \mapsto u = u(h), h > 0$, are strictly concave and strictly

decreasing functions. The projection of the wave curve $\mathcal{W}_3(U_0)$ in the (h, u)-plane can be parameterized as $h \mapsto u = u(h), h > 0$, which is a strictly convex and strictly decreasing function for $u_0 > 0$ and strictly concave and strictly increasing function for $u_0 < 0$.

In the case (ii), the discontinuity satisfies

$$\begin{aligned} &[hu] = 0, \\ &[\tfrac{u^2}{2} + g(h+a)] = 0. \end{aligned} \tag{14}$$

The relations (14) define the stationary-wave curve parameterized by h:

$$\mathcal{W}_3(U_0): \quad \begin{aligned} u = u(h) &= \tfrac{h_0 u_0}{h}, \\ a = a(h) &= a_0 + \tfrac{u_0^2 - u^2}{2g} + h_0 - h. \end{aligned} \tag{15}$$

The above arguments show that *the a-component of Riemann solutions may change only across a stationary wave.* This is important for the discretization of the source terms later on.

2.2. Equilibrium states

Given a state $U_0 = (h_0, u_0, a_0)$ and a bottom level $a \neq a_0$. Let $U = (h, u, a)$ be the corresponding right-hand state of the stationary contact issuing from the given left-hand state U_0. We need to find out h and u in terms of U_0 and a. Multiplying both sides of the second equation of (21) and using the first equation, we find that h is the root of the nonlinear equation

$$\varphi(h) = \varphi(U_0, a; h) = 2gh^3 + (2g(a-a_0-h_0) - u_0^2)h^2 + h_0^2 u_0^2 = 0, \quad h > 0. \tag{16}$$

We have
$$\begin{aligned} \varphi(0) &= h_0^2 u_0^2 \geq 0, \\ \varphi'(h) &= 6gh^2 + 2(2g(a - a_0 - h_0) - u_0^2)h, \\ \varphi''(h) &= 12gh + 2(2g(a - a_0 - h_0) - u_0^2). \end{aligned}$$

Thus,

$$\varphi'(h) = 0 \quad \text{iff} \quad h = 0, \quad \text{or} \quad h = h_* = h_*(U_0, a) := \frac{u_0^2 + 2g(a_0 + h_0 - a)}{3g}. \tag{17}$$

If $h_*(U_0, a) < 0$, or $a > a_0 + h_0 + \tfrac{u_0^2}{2g}$, then $\varphi'(h) > 0$ for $h > 0$. Since $\varphi(0) = h_0^2 u_0^2 \geq 0$, there is no root for (16) if (17) holds. Otherwise, if

$$a \leq a_0 + h_0 + \frac{u_0^2}{2g},$$

7

then $\varphi' > 0$ for $h > h_*$ and $\varphi'(h) < 0$ for $0 < h < h_*$. In this case, φ admits a zero $h > 0$, and in this case it has two zeros, iff

$$\varphi_{\min} := \varphi(h_*) = -gh_*^3 + h_0^2 u_0^2 \leq 0,$$

or

$$h_*(U_0, a) \geq h_{\min}(U_0) := \left(\frac{h_0^2 u_0^2}{g}\right)^{1/3}, \tag{18}$$

where h_* is defined by (17). It is easy to check that (18) holds if and only if

$$
\begin{aligned}
a \leq a_{\max}(U_0) \quad &:= a_0 + h_0 + \frac{u_0^2}{2g} - \frac{3}{2g^{1/3}}(h_0 u_0)^{2/3} \\
&= a_0 + \frac{1}{2g}((gh_0)^{1/3} - u_0^{2/3})^2 (2(gh_0)^{1/3} + u_0^{2/3}).
\end{aligned}
\tag{19}
$$

Observe that (19) implies $a_{\max}(U_0) \geq a_0$ and the equality holds only if (h_0, u_0) belongs to the surfaces $\mathcal{C}_\pm$. Whenever (19) is fulfilled, the function φ in (16) admits two root denoted by $h_1(a) \leq h_2(a)$ satisfying $h_1(a) \leq h_* \leq h_2(a)$. Moreover, if the inequality in (19) is strict, i.e., $a < a_{\max}(U_0)$, then these two roots are distinct: $h_1(a) < h_* < h_2(a)$. Thus, we arrive at the following lemma.

Lemma 2.1. *Given $U_0 = (h_0, u_0, a_0)$ and a bottom level $a \neq a_0$. The following conclusions holds.*

(i)

$$a_{\max}(U_0) \geq a_0, \quad a_{\max}(U_0) = a_0 \quad \text{if and only if} \quad (h_0, u_0) \in \mathcal{C}.$$

(ii) *The nonlinear equation (16) admits a root if and only if the condition (19) holds, and in this case it has two roots $h_1(a) \leq h_* \leq h_2(a)$. Moreover, whenever the inequality in (19) is strict, i.e. $a < a_{\max}(U_0)$, these two roots are distinct.*

(iii) *According to the part (ii), whenever (19) is fulfilled, there are two states $U_i(a) = (h_i(a), u_i(a), a)$,, where $u_i(a) = h_0 u_0 / h_i(a), i = 1, 2$ to which a stationary contact from U_0 is possible. Moreover, the locations of these states can be determined as follows*

$$
\begin{aligned}
U_1(a) &\in G_1 \quad \text{if} \quad u_0 > 0, \\
U_1(a) &\in G_3 \quad \text{if} \quad u_0 < 0, \\
U_2(a) &\in G_2.
\end{aligned}
$$

Proof. The parts (i) and (ii) can be easily deduced from the above argument. To prove (iii), it is sufficient to show that along the projection of $\mathcal{W}_3(U_0)$ on the (h, u)-plane, the point $U_{\min}(U_0) = (h_{\min}(U_0), u_{\min}(U_0) := h_0 u_0 / h_{\min}(U_0))$, where $h_{\min}(U_0)$ is defined by (18), belongs to $\mathcal{C}_+$ if $u_0 > 0$ and belongs to $\mathcal{C}_-$ if $u_0 < 0$, and that $U_i(a) \in \mathcal{W}_3(U_0), i = 1, 2$, such that $U_2(a) \in G_2$ and $U_1(a)$ is located on the other side of $U_1(a)$ with respect to $\mathcal{C}$. Indeed, let us define a function taking values along the stationary curve $\mathcal{W}_3(U_0)$:

$$\sigma(h) := u(h)^2 - gh = \frac{h_0^2 u_0^2}{h^2} - gh.$$

Clearly, a point $U = (h, u, a)$ belongs to $G_1 \cup G_3$ if and only if $\sigma(h) > 0$ and U belongs to G_2 if and only if $\sigma(h) < 0$. Since $\sigma(h_{\min}(U_0)) = 0$, the point $U_{\min}(U_0)$ belongs to Obviously, $U_{\min}(U_0) \in \mathcal{C}_+$ if $u_0 > 0$, and $U_{\min}(U_0) \in \mathcal{C}_-$ if $u_0 < 0$. Thus, we have left to prove that

$$\sigma(h_1(a)) > 0, \quad \sigma(h_2(a)) < 0. \tag{20}$$

Since
$$\sigma(h_{\min}(U - 0)) = 0, \quad \sigma'(h) = \frac{-2h_0^2 u_0^2}{h^3} - g < 0,$$

we can see that (20) holds if

$$h_1(a) < h_{\min}(U_0) < h_2(a). \tag{21}$$

On the other hand, we have

$$\begin{aligned} \varphi(h) &> 0, \quad \text{if } h < h_1(a) \quad \text{or} \quad h > h_2(a), \\ \varphi(h) &< 0, \quad \text{if } h_1(a) < h < h_2(a). \end{aligned} \tag{22}$$

And we have

$$\varphi(h_{\min}(U_0)) = 3(h_0 u_0)^2 + (2g(a - a_0 - h_0) - u_0^2)\frac{(h_0 u_0)^{4/3}}{g^{2/3}}.$$

It is a straightforward calculation to show that the condition

$$a < a_{\max}(U_0)$$

is equivalent to

$$\varphi(h_{\min}(U_0)) < 0.$$

9

This together with (22) establish (21). Lemma 2.1 is completely proved. □

From Lemma 2.1, we can construct two-parameter wave sets. The Riemann problem for (1) may therefore admit up to a one-parameter family of solutions. To select a unique Riemann solution, we impose an admissibility condition for stationary contacts, known as the *monotonicity criterion*, as follows

(MC) (Monotonicity Criterion) Along any stationary curve $\mathcal{W}_3(U_0)$, the bottom level a is monotone as a function of h. The total variation of the bottom level component of any Riemann solution must not exceed $|a_L - a_R|$, where a_L, a_R are left-hand and right-hand cross-section levels.

A similar criterion was used by Isaacson and Temple Isaacson and Temple (1992, 1995) and by LeFloch and Thanh LeFloch and Thanh (2003), and by Goatin and LeFloch GoatinLeFloch (2004).

Lemma 2.2. *The Monotonicity Criterion implies that any stationary shock does not cross the boundary of strict hyperbolicity. In other words:*

(i) *If $U_0 \in G_1 \cup G_3$, then only the stationary shock based on the value $h_1(a)$ is allowed, and we set $\bar{h}(a) = h_1(a)$.*

(ii) *If $U_0 \in G_2$, then only the stationary shock using $h_2(a)$ is allowed, and we set $\bar{h}(a) = h_2(a)$.*

Thus, $\bar{h}(a)$ is the admissible h-value of a right-hand state $U = (h = \bar{h}(a), u, a)$ of the stationary wave from a given left-hand state $U_0 = (h_0, u_0, a_0)$.

Proof. Recall that the Rankine-Hugoniot relations associate the linearly degenerate field (14) implies that the component a can be expressed as a function of h:

$$a = a(h) = a_0 + \frac{-u^2 + u_0^2}{2g} - h + h_0,$$

where

$$u = u(h) = \frac{h_0 u_0}{h}.$$

Thus, taking the derivative of a with respect to h, we have

$$\begin{aligned} a'(h) &= \frac{-u u'(h)}{g} - 1 = u \frac{h_0 u_0}{gh^2} - 1 \\ &= \frac{u^2}{gh} - 1 = \frac{(u^2 - gh)}{gh} \end{aligned}$$

which has the same sign as $u^2 - gh$. Thus, $a = a(h)$ is increasing with respect to h in the domains G_1, G_3 and is decreasing in the domain G_2. Thus, in order that $a = a(h)$ is monotone as a function of h, the point (h, u, a) must stay in the closure of the domain containing (h_0, u_0, a_0). The conclusions of (i) and (ii) then follow. □

How to compute the roots of the equation (16)? The above argument shows that whenever (19) is satisfied, the equation (16) admits two roots $h_1(a), h_2(a)$ satisfying

$$h_1(a) \leq h_{\min} = \left(\frac{h_0^2 u_0^2}{g}\right)^{1/3} \leq h_* = \frac{u_0^2 + 2g(a_0 + h_0 - a)}{3g} \leq h_2(a) \qquad (23)$$

and the inequalities are all strict whenever the inequality in (19) is strict. Since $0 < h_1(a) \leq h_{\min} \leq h_*$ and

$$\varphi(0) \geq 0,$$
$$\varphi(h_*) \leq 0, \varphi(h_{\min}) \leq 0,$$

the root $h_1(a)$ of (16) can be computed using the regula falsi method with the starting interval $[0, h_{\min}]$, or $[0, h_*]$. And since $h_2(a) \geq h_*$ and $\varphi'(h) > 0, \varphi''(h) > 0, h > h_*$, the root $h_2(a)$ can be computed using Newton's method with any starting point larger than h_*. We summarize this in the following lemma.

Lemma 2.3. (Finding the water height of stationary contacts) *The root $h_1(a)$ of (16) can be computed using the regula falsi method for the starting interval $[0, h_{\min}]$, where $h_{\min} = \left(\frac{h_0^2 u_0^2}{g}\right)^{1/3}$, or $[0, h_*]$, where $h_* = \frac{u_0^2 + 2g(a_0 + h_0 - a)}{3g}$, while the root $h_2(a)$ can be computed using Newton's method with any starting point larger than h_*.*

3. The Riemann problem revisited

From the general theory of nonconservative systems of balance laws, it is known that if Riemann data belongs to a sufficiently small ball in a strictly hyperbolic region, then the Riemann problem admits a unique solution. It is worth to note that this result no longer holds if any of these assumptions fails due to the resonance.

Our goal in this section to to provide all possible explicit constructions for Riemann solutions, investigating when Riemann data are distributed around

11

the strictly hyperbolic boundary $\mathcal{C}_\pm$. There are several improvements in the constructions of Riemann solutions in this paper over the ones in our previous work LeFloch and Thanh (2007). First, we can determine larger domains of existence by combining constructions in LeFloch and Thanh (2007) together due to connectivity. Second, the domains where there is a unique solution or there are several solutions are estimated. Under the transformation $x \mapsto -x, u \mapsto -u$, a left-hand state $U = (h, u, a)$ in G_2 or G_3 will be transferred to the right-hand state $V = (h, -u, a)$ G_2 or G_1, respectively. Thus, the construction for Riemann data around $\mathcal{C}_-$ can be obtained from the one for Riemann data around $\mathcal{C}_+$. We thus construct only the case where Riemann data are in $G_1 \cup \mathcal{C}_+ \cup G_2$ and we separate into two regimes on which a corresponding construction based on the left-hand state U_L is given:

- *Regime (A): $U_L \in G_1 \cup \mathcal{C}_+$;*

- *Regime (B): $U_L \in G_2$;*

For each construction, depending on the location of the right-hand states U_R and the sign $a_R - a_L$ there will be different types of solutions or the results on the existence and uniqueness.

As in LeFloch and Thanh (2007), to construct Riemann solutions of (1)-(2), we project all the wave curves on the (h, u)-plane using the following notations:

(i) U^0 denotes the state resulted from a stationary contact wave from U;

(ii) $W_k(U_i, U_j)$ $(S_k(U_i, U_j), R_k(U_i, U_j))$ denotes the kth-wave (kth-shock, kth-rarefaction wave, respectively) connecting the left-hand state U_i to the right-hand state U_j, $k = 1, 2, 3$;

(iii) $W_m(U_i, U_j) \oplus W_n(U_j, U_k)$ indicates that there is an mth-wave from the left-hand state U_i to the right-hand state U_j, followed by an nth-wave from the left-hand state U_j to the right-hand state U_k, $m, n \in \{1, 2, 3\}$.

3.1. Regime (A): Eigenvalues at U_L have the same sign

Let $\bar{G}_1$ denote the closure of G_1. We assume that $U_L \in \bar{G}_1$, or equivalently $\lambda_i(U_L) \geq 0, i = 1, 2, 3$.

Lemma 3.1. *Consider the projection on the (h, u)-plan. To every $U = (h, u) \in G_1$ there exists exactly one point $U^{\#} \in \mathcal{S}_1(U) \cap G_2+$ such that the 1-shock speed $\bar{\lambda}_1(U, U^{\#}) = 0$. The state $U^{\#} = (h^{\#}, u^{\#})$ is defined by*

$$h^{\#} = \frac{-h + \sqrt{h^2 + 8hu^2/g}}{2}, \quad u^{\#} = \frac{uh}{h^{\#}}.$$

Moreover, for any $V \in \mathcal{S}_1(U)$, the shock speed $\bar{\lambda}_1(U, V) > 0$ if and only if V is located above $U^{\#}$ on $\mathcal{S}_1(U)$.

Construction (A1). In this case (the projection on (h, u)-plane of) U_R is located in a "higher" region containing U_L in the (h, u)-plane. See Figure 1.

If $a_L \geq a_R$ (or $a_L < a_R \leq a_{\max}(U_L)$), the solution begins with a stationary contact upward (downward, respectively) along $\mathcal{W}_3(U_L)$ from U_L to the state $U_L^o \in \mathcal{W}_3(U_L) \cap G_1$, shifting the level a_L directly to the level a_R. Let

$$\{U_M = (h_M, u_M, a_R)\} = \mathcal{W}_1(U_L^o) \cap \mathcal{W}_2^B(U_R).$$

Providing that $\lambda_1(U_L^o, U_M) \geq 0$, or equivalently, as seen from Lemma 3.1, $h_M \leq h_L^{o\#}$, the solution can continue by a 1-wave from U_L^o to U_M, followed by a 2-wave from U_M to U_R. Thus, the solution is

$$W_3(U_L, U_L^o) \oplus W_1(U_L^o, U_M) \oplus W_2(U_M, U_R). \tag{24}$$

This construction can be extended if $\mathcal{W}_2^B(U_R)$ lies entirely above $\mathcal{W}_1(U_L^o)$. In this case let I and J be the intersection points of $\mathcal{W}_1(U_L^o)$ and $\mathcal{W}_2^B(U_R)$ with the axis $\{h = 0\}$, respectively:

$$\{I\} = \mathcal{W}_1(U_L^o) \cap \{h = 0\}, \quad \{J\} = \mathcal{W}_2^B(U_R) \cap \{h = 0\}, \tag{25}$$

then the solution can be seen as a dry part $W_o(I, J)$ between I and J. Thus, the solution in this case is

$$W_3(U_L, U_L^o) \oplus R_1(U_L^o, I) \oplus W_o(I, J) \oplus R_2(J, U_R).$$

Remark 1. As seen by Lemma 2.1, if $a_L < a_R$, the condition

$$a_R \leq a_{\max}(U_L)$$

is necessary for the stationary contact $W_3(U_L, U_L^o)$. Therefore, if this condition fails, there is no solution even if $U_L = U_R$. The necessary and sufficient conditions for the existence of the solution (24) is that $U_L^{o\#}$ is located below or on the curve $\mathcal{W}_2^B(U_R)$. This domain clearly covers a large crossing-strictly-hyperbolic-boundary neighborhood of U_L.
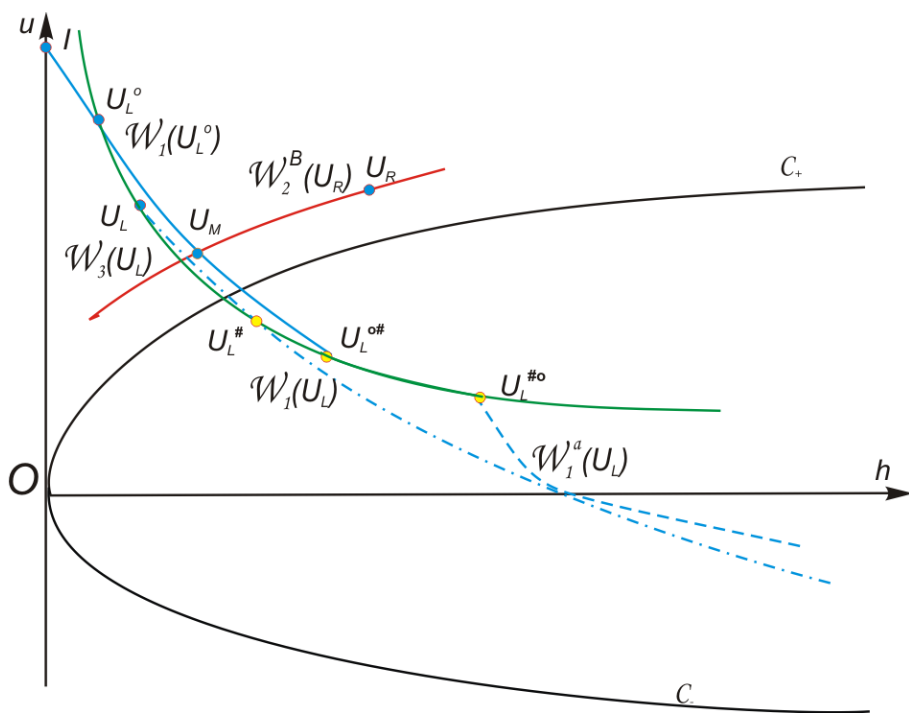
Figure 1: Construction (A1), $a_L > a_R$: A solution of the form (24)

Construction (A2). Roughly speaking, this case concerns with the fact that $\overline{U_R}$ moves limitedly downward from the case G_1. Instead of using "complete" stationary contact from U_L to U_L^o as in the first possibility, the solution now begins with a "half-way" stationary contact $W_3(U_L, U_1)$ from $U_L = (h, u, a_L)$ to some state $U_1 = U_L^o(a) = (h, u, a) \in \mathcal{W}_3(U_L)$, where a between a_L and a_R. The solution then continues by a 1-shock wave with zero speed from U_1 to $U_2 = U_1^\# \in \mathcal{W}_1(U_1) \cap G_2$. Observe that U_2 still belongs to $\mathcal{W}_3(U_L)$, since $h_2 u_2 = h_1 u_1 = h_L u_L$, as indicated by Lemma 3.1. The solution continues by a stationary contact from U_2 to a state $U_M(a) \in \mathcal{W}_3(U_L)$. The set of these points $U_M(a), a \in [a_L, a_R]$ forms a curve pattern denoted by $\mathcal{L}$. Whenever

$$\mathcal{W}_2^B(U_R) \cap \mathcal{L} \neq \emptyset$$

there is a solution containing three discontinuities having the same zero speed of the form

$$W_3(U_L, U_1) \oplus S_1(U_1, U_2) \oplus W_3(U_2, U_M) \oplus W_2(U_M, U_R). \tag{26}$$

See Figure 2.

Remark 2. The necessary and sufficient conditions for the existence of the solution (26) is that $U_L^{o\#}$ is located above or on the curve $\mathcal{W}_2^B(U_R)$, and $U_L^{\#o}$ is located below or on the curve $\mathcal{W}_2^B(U_R)$. This domain covers a region in G_2+ and G_1 which is "quite far away" from U_L.

It is interesting that at the limit $a = a_R$ at the first jump, we get the first possibility. If $a = a_L$, then the solution simply begins with a 1-shock wave with zero speed followed by a stationary contact shifting a from a_L to a_R. This limit case can be connected to the following possibility.

Construction (A3). The solution begins with a strong 1-shock wave from U_L to any state $U \in \mathcal{W}_1(U_L) \cap G_2$ such that $\lambda_1(U_L, U) \leq 0$. This shock wave is followed by a stationary contact to a state U^o shifting a from a_L to a_R. The set of these states U^o form a curve denoted by $\mathcal{W}_1^a(U_L)$. Whenever

$$\emptyset \neq \mathcal{W}_2^B(U_R) \cap \mathcal{W}_1^a(U_L) = \{U_M^o\} \in G_2, \quad \text{and} \quad \bar{\lambda}_2(U_M^o, U_R) \geq 0, \tag{27}$$

there will be a Riemann solution defined by

$$S_1(U_L, U_M) \oplus W_3(U_M, U_M^o) \oplus W_2(U_M^o, U_R). \tag{28}$$
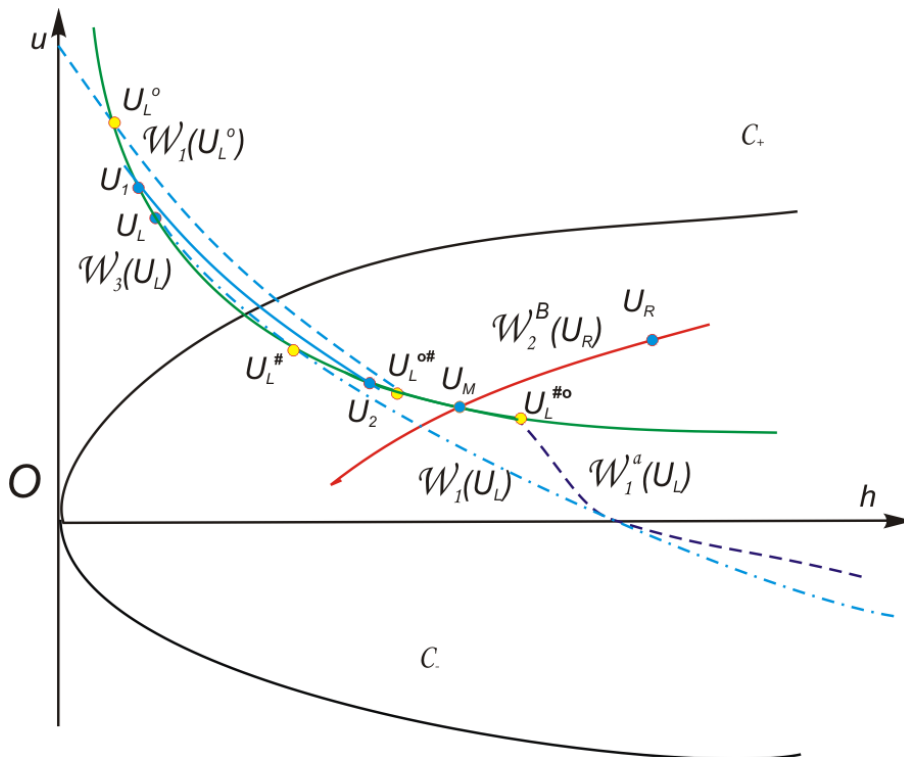
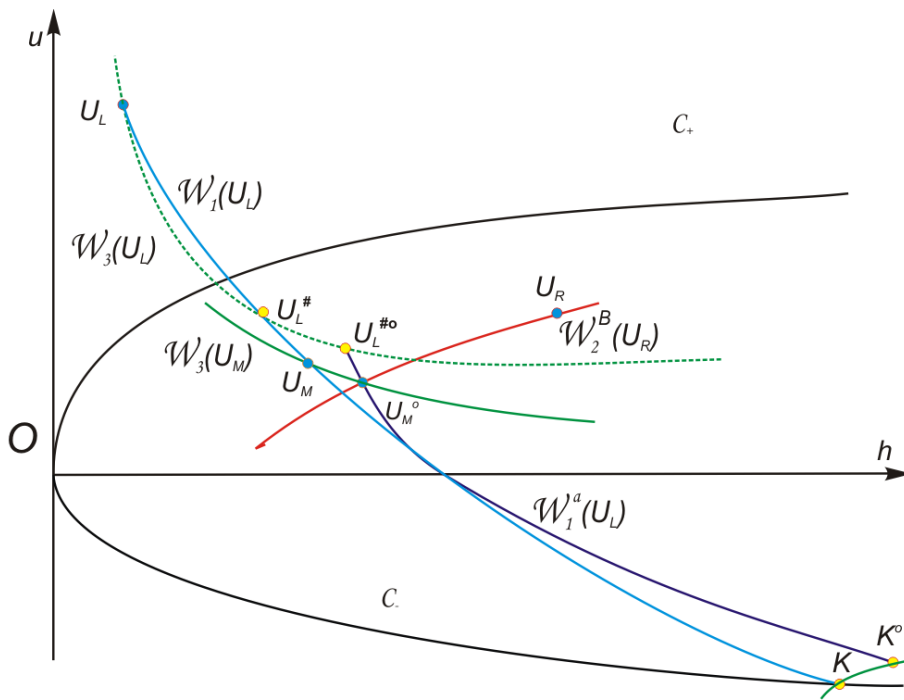Figure 2: Construction (A2), $a_L > a_R$: A solution of the form (26)

16

Figure 3: Construction (A3), $a_L > a_R$: A solution of the form (28)

In the limit case of (26) where $U_1 \equiv U_L$, the solution (26) coincides with the solution (28). See Figure 3.

Let K denote the lower limit state on $\mathcal{W}_1(U_L)$ that the solution (28) makes sense, and let $K^o \in G_2$ denote the right-hand state resulted from a stationary contact from K shifting a_L to a_R. Thus, we have

$$\begin{aligned} \{K\} &= \mathcal{W}_1(U_L) \cap \mathcal{C}_-, \quad \text{if } a_L \geq a_R, \\ \{K\} &\in \mathcal{W}_1(U_L) \quad \text{such that } a_{\max}(K) = a_R, \quad \text{if } a_L < a_R. \end{aligned} \tag{29}$$

Remark 3. The solution (28) makes sense if $U_L^{\#o}$ is above or on the curve $\mathcal{W}_2^B(U_R)$, and K^o lies below or on the curve $\mathcal{W}_2^B(U_R)$ and $\bar{\lambda}_3(K^o, U_R) \geq 0$.

The union of the wave patterns $\mathcal{W}_1(U_1) \cup \mathcal{L} \cup \mathcal{W}_1^a(U_L)$ form a continuous curve. The Riemann problem thus admits a solution whenever $\mathcal{W}_2^B(U_R)$ intersects $\mathcal{W}_1(U_1) \cup \mathcal{L} \cup \mathcal{W}_1^a(U_L)$ or $\mathcal{W}_2^B(U_R)$ intersects with $\{h = 0\}$ at a point above the point I. We can see that this happens for a large domain of U_R containing U_L. See Figures 1, 2, and 3.

If the wave pattern $\mathcal{L}$ lies entirely on one side with respect to the curve $\mathcal{W}_2^B(U_R)$, then $\mathcal{W}_2^B(U_R)$ intersects either $\mathcal{W}_1(U_1)$ or $\mathcal{W}_1^a(U_L)$ at most one point. Therefore, then (24) or (28) is the *unique solution*. Besides, if $\mathcal{W}_2^B(U_R)$ intersects the wave pattern $\mathcal{L}$, and if $h_L^{\#o} \geq h_L^{o\#}$, then the point $U_L^{\#o}$ is located below the point $U_L^{o\#}$ on the curve $\mathcal{W}_3(U_L)$. Thus, the curve $\mathcal{W}_2^B(U_R)$ does not meet $\mathcal{W}_1(U_1)$ nor $\mathcal{W}_1^a(U_L)$, except possibly at the endpoints $U_L^{\#o} \in \mathcal{L}$ and $U_L^{o\#} \in \mathcal{L}$. In this case, (26) is the sole solution. In summary, the Riemann problem for (1)-(2) always *has at most one solution* whenever $h_L^{\#o} \geq h_L^{o\#}$.

In the case where $h_L^{\#o} < h_L^{o\#}$, *there can be three solutions*, as $\mathcal{W}_2^B(U_R)$ can meet all the three curve patterns $\mathcal{W}_1(U_1), \mathcal{L}$ and $\mathcal{W}_1^a(U_L)$, or

$$h_L^{\#o} < h_L^{o\#}, \quad \Phi_2(U_L^{\#o}; U_R) > 0 > \Phi_2(U_L^{o\#}; U_R), \tag{30}$$

where the function $\Phi_2(U; U_R)$ is defined by (13). See Figure 4.

The above argument leads us to the following theorem.

Theorem 3.2 (Riemann problem for shallow water equations). *Given a left-hand state $U_L \in G_1$. Depending on the location of the right-hand state U_R we have the following conclusions.*

(a) **Existence.** *The Riemann problem (1)-(3) admits a solution if Q^o defined in Construction (A3) lies below or on the curve $\mathcal{W}_2^B(U_R)$, and that if $\mathcal{W}_2^B(U_R)$ intersects with $\mathcal{W}_1^a(U_L)$ at some point $U_M^o \in G_1-$, then $\bar{\lambda}_2(U_M^o, U_R) \geq 0$.*
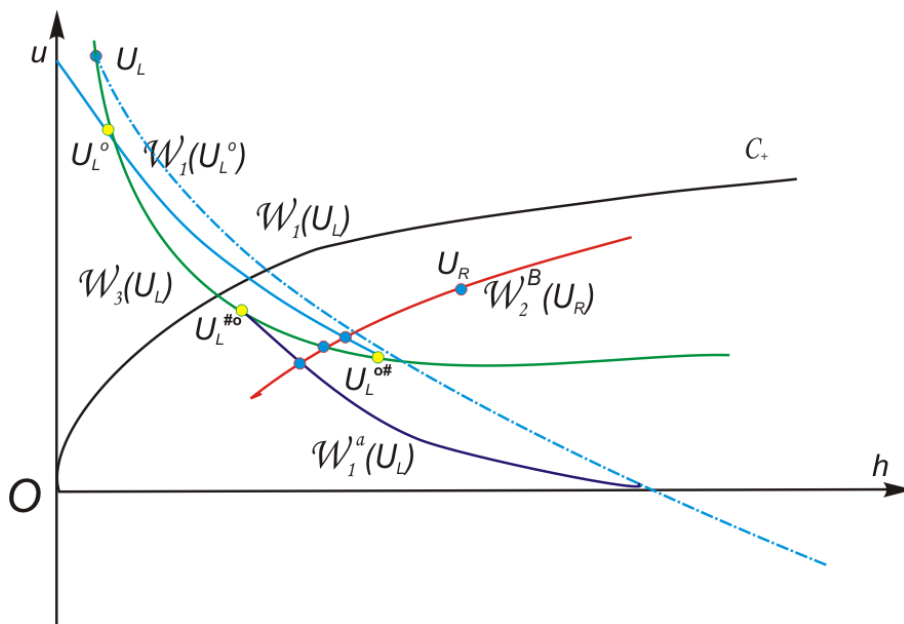
18

Figure 4: Non-uniqueness: Three admissible Riemann solutions of the form (24), (26), and (28)

(b) **Regime of uniqueness.** *The Riemann problem (1)-(3) has at most one solution if*

– either $h_L^{\#o} \geq h_L^{o\#}$;

– or $h_L^{\#o} < h_L^{o\#}$, and the states $U_L^{\#o}$ and $U_L^{o\#}$ are located on the same side with respect to the curve $\mathcal{W}_2^B(U_R)$.

(c) **Multiple solutions.** *If $h_L^{\#o} < h_L^{o\#}$, and if the state $U_L^{\#o}$ lies above the curve $\mathcal{W}_2^B(U_R)$ while the state $U_L^{o\#}$ lies below the curve $\mathcal{W}_2^B(U_R)$, then the Riemann problem (1)-(3) has three solutions.*

Example. We provide some numerical experiments to illustrate two situations: $h_L^{\#o} > h_L^{o\#}$, and $h_L^{\#o} < h_L^{o\#}$ corresponding to the two cases $a_L > a_R$ (see Tables A1-A3) and $a_L < a_R$ (see Tables A4, A5). We take at random the state U_L and a_R.

(a) $a_L > a_R$: all experiments show that $h_L^{\#o} > h_L^{o\#}$. In Table A1, $U_L \in G_1$.

Table A1			
States	U_L	$U_L^{\#o}$	$U_L^{o\#}$
Water Height h	0.5	1.1930011	1.1171275
Velocity u	4	1.6764444	1.790306
Bottom Level a	1	0.9	0.9

In Table A2, $U_L \in \mathcal{C}_+$.

Table A2			
States	U_L	$U_L^{\#o}$	$U_L^{o\#}$
Water Height h	1	1.3075478	1.2558035
Velocity u	3.1304952	2.3941726	2.4928225
Bottom Level a	1	0.9	0.9

In Table A3, $U_L \in G_1$ is far away from $\mathcal{C}_+$.

Table A3			
States	U_L	$U_L^{\#o}$	$U_L^{o\#}$
Water Height h	0.01	0.54763636	0.44902891
Velocity u	10	0.18260292	0.22270281
Bottom Level a	1	0.9	0.9

(b) $a_L < a_R$: all experiments show that $h_L^{\#o} < h_L^{o\#}$. In Table A4, $U_L \in G_1$.

Table A4			
States	U_L	$U_L^{\#o}$	$U_L^{o\#}$
Water Height h	0.5	0.86127059	0.96534766
Velocity u	4	2.3221506	2.0717925
Bottom Level a	0.9	1	1

In Table A5, $U_L \in G_1$ is far away from $\mathcal{C}_+$.

Table A5			
States	U_L	$U_L^{\#o}$	$U_L^{o\#}$
Water Height h	0.01	1.2748668	1.3718425
Velocity u	10	0.78439566	0.72894668
Bottom Level a	0.9	1	1

Remark 4. We conjecture that if $a_L > a_R$, then $h_L^{\#o} > h_L^{o\#}$, and if $a_L < a_R$, then $h_L^{\#o} < h_L^{o\#}$. If this conjecture is verified, then Theorem 3.2 implies that when $a_L \geq a_R$, the Riemann problem always has at most one solution for $U_L \in G_1$.

3.2. Regime (B): Eigenvalues at U_L have opposite signs

In this subsection we consider the case where the left-hand state U_L moves downward from the Regime (A): $U_L \in \bar{G}_2$, or $\lambda_1(U_L) < 0 = \lambda_3(U_L) < \lambda_2(U_L)$.
Construction (B1). For U_R in a "higher" position, there can be two types of solutions depending on whether $a_L \geq a_R$.

If $a_L > a_R$ a solution can be constructed as follows. The solution begins from U_L with a 1-rarefaction wave until it reaches $\mathcal{C}_+$ at a state $U_1 \in \mathcal{W}_1(U_L) \cap \mathcal{C}_+$. A straightforward calculation gives

$$U_1 = \left((\frac{u_L}{3\sqrt{g}} + \frac{2}{3}\sqrt{h_L})^2, \frac{1}{3}u_L + \frac{2}{3}\sqrt{gh_L}, a_L \right).$$

This rarefaction wave can be followed by a stationary jump $W_3(U_1, U_2)$ into G_1. This stationary wave is possible since $a_L \geq a_R$. Let $\{U_3\} = \mathcal{W}_1(U_2) \cap \mathcal{W}_2^B(U_R)$. The solution is then continued by a 1-wave from U_2 to U_3, followed by a 2-wave from U_3 to U_R. Thus, the solution is given by the formula

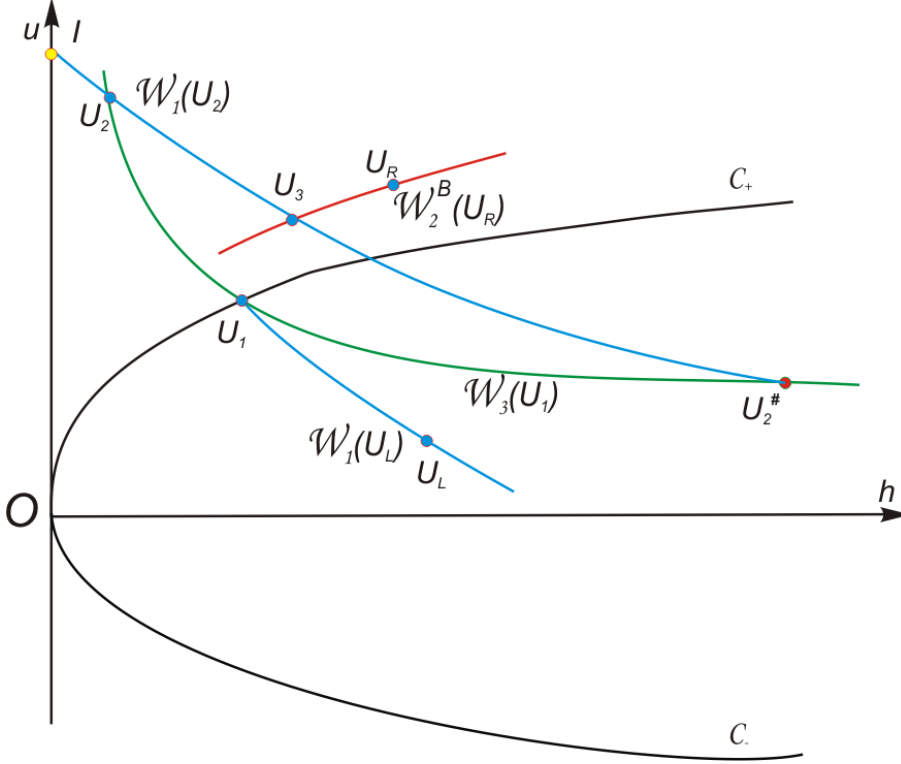$$R_1(U_L, U_1) \oplus W_3(U_1, U_2) \oplus W_1(U_2, U_3) \oplus W_2(U_3, U_R). \tag{31}$$

Figure 5: Construction (B1), $a_L > a_R$: A solution of the form (31)

The construction makes sense if $\bar{\lambda}_1(U_2, U_3) \geq 0$, which means U_3 has to be above $U_2^{\#}$ on $\mathcal{W}_1(U_2)$. This construction can also be extended if $\mathcal{W}_2^B(U_R)$ lies entirely above $\mathcal{W}_1(U_2)$. In this case let I and J be the intersection points of $\mathcal{W}_1(U_2)$ and $\mathcal{W}_2^B(U_R)$ with the axis $\{h = 0\}$, respectively:

$$\{I\} = \mathcal{W}_1(U_2) \cap \{h = 0\}, \quad \{J\} = \mathcal{W}_2^B(U_R) \cap \{h = 0\}. \tag{32}$$

Then, the solution can be seen as containing a dry part $W_o(I, J)$ between I and J. Thus, the solution in this case is

$$R_1(U_L, U_1) \oplus W_3(U_1, U_2) \oplus W_1(U_2, I) \oplus W_o(I, J) \oplus R_2(J, U_R).$$

See Figure 5.

If $a_L \leq a_R$ a solution of another type can be constructed as follows. To each $U \in \mathcal{C}_+$, a stationary contact to $U^o \in G_2$ downing $a = a_R$ to $a = a_L$ is

22

possible, since $a_R > a_L$. The set of all these states U^o form a curve denoted by $\mathcal{C}_+^a$. Let

$$\{U_1\} = \mathcal{W}_1(U_L) \cap \mathcal{C}_+^a.$$

Then, the solution begins by a 1-wave $W_1(U_L, U_1)$, followed by a stationary jump $W_3(U_1, U_2 = U_1^o)$ to $U_2 \in \mathcal{C}_+$. Let $\{U_3\} = \mathcal{W}_1(U_2) \cap \mathcal{W}_2^B(U_R)$. The solution is then continued by a 1-rarefaction wave from U_2 to U_3, followed by a 2-wave from U_3 to U_R. Thus, the solution is given by the formula

$$W_1(U_L, U_1) \oplus W_3(U_1, U_2) \oplus R_1(U_2, U_3) \oplus W_2(U_3, U_R). \qquad (33)$$

The construction makes sense if $\lambda_1(U_3) \geq 0$, or $U_3 \in \bar{G}_1$. This construction can also be extended if $\mathcal{W}_2^B(U_R)$ lies entirely above $\mathcal{W}_1(U_2)$. In this case let I and J be the intersection points of $\mathcal{W}_1(U_2)$ and $\mathcal{W}_2^B(U_R)$ with the axis $\{h = 0\}$, respectively:

$$\{I\} = \mathcal{W}_1(U_2) \cap \{h = 0\}, \quad \{J\} = \mathcal{W}_2^B(U_R) \cap \{h = 0\}. \qquad (34)$$

Then, the solution can be seen as containing a dry part $W_o(I, J)$ between I and J. Thus, the solution in this case is

$$W_1(U_L, U_1) \oplus W_3(U_1, U_2) \oplus R_1(U_2, I) \oplus W_o(I, J) \oplus R_2(J, U_R).$$

See Figure 6.

The wave structure of the solutions (31) and (32) are the same, but the state at which the solution reaches the strictly hyperbolic boundary $\mathcal{C}$ using a different wave. However, one may argue that in both cases the solution uses a stationary contact to reach $\mathcal{C}_+$ from either side of $\mathcal{C}_+$. Moreover, all the states in the solution $(U_L, U_1, U_2, U_3, U_R)$ can be in an arbitrarily small ball center on $\mathcal{C}_+$.

Construction (B2). This case holds only when $a_L > a_R$, where there is an interesting phenomenon as wave speeds associate with different characteristic fields coincide and all equal zero. The solution therefore contain three waves with the same zero speed.

The solution begins with a 1-rarefaction wave until it reached $\mathcal{C}_+$ at U_1. At U_1, the solution may jump to G_1 using a "half-way" stationary wave to a state $M = M(a) = U_1^o(a)$ from the bottom height a_L to any $a \in [a_R, a_L]$. Then, the solution can continue by a 1-shock with zero speed from M to $N = N(a) = N^\#(a) \in G_2^+$, followed by a stationary wave from N to $P = P(a) = N^o(a)$ with a shift in a-component from a to a_R. The set of these states $P(a)$ form
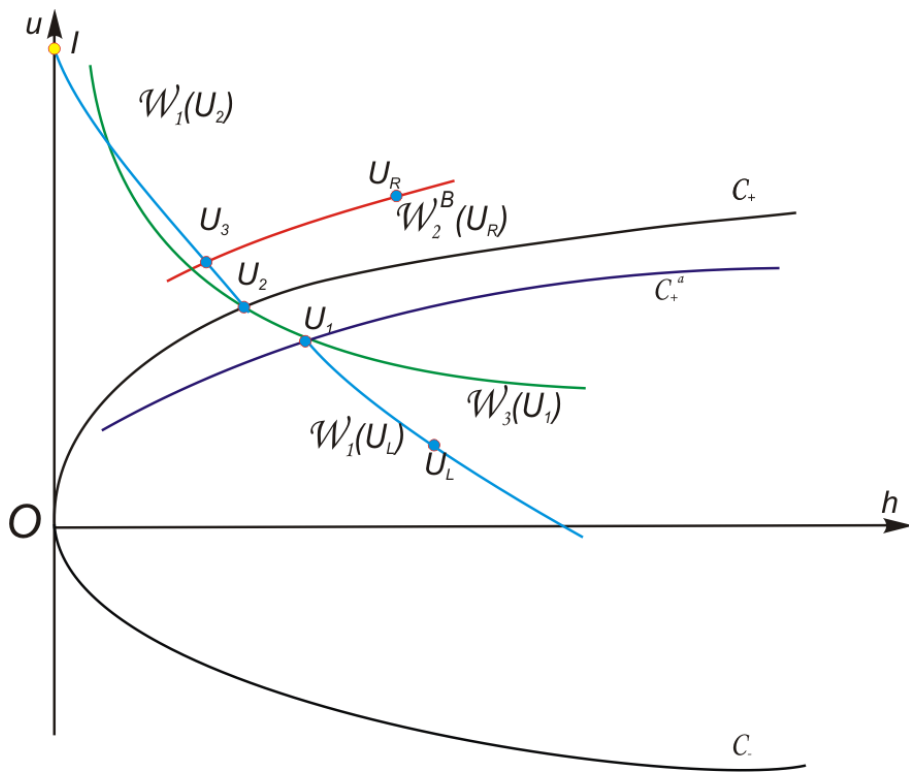
23

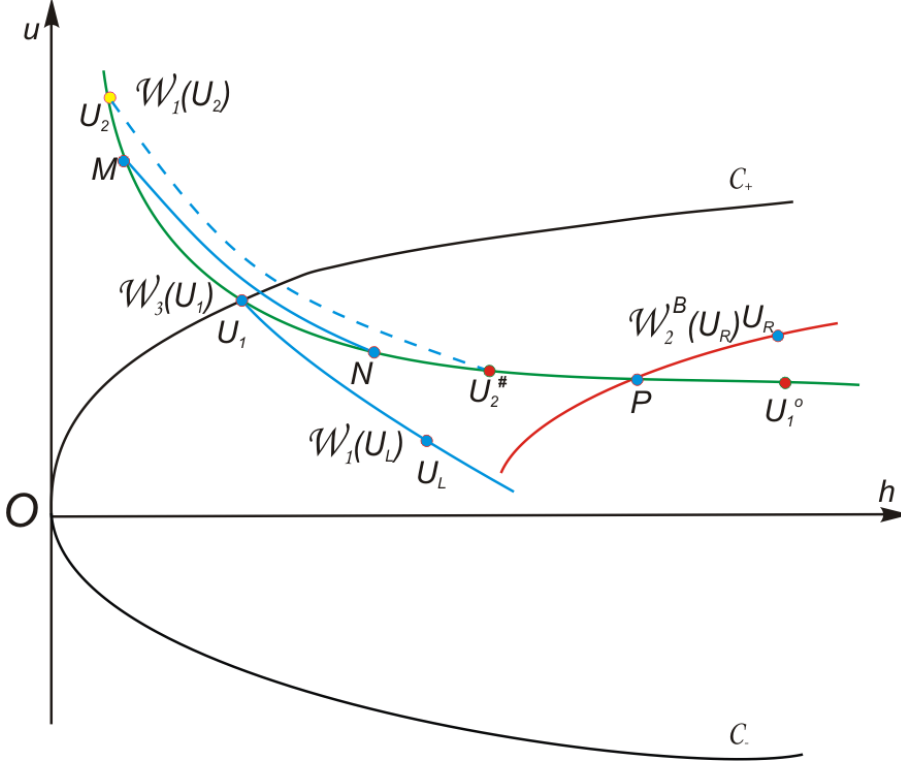Figure 6: Construction (B1), $a_L \leq a_R$: A solution of the form (32)

Figure 7: Construction (B2), $a_L > a_R$: A solution of the form (35)

a curve pattern $\mathcal{L}$. So, whenever $\emptyset \neq \mathcal{W}_2^B(U_R) \cap \mathcal{L} = \{P = P(a)\}$, there is a Riemann solution containing three zero-speed waves of the form

$$R_1(U_L, U_1) \oplus W_3(U_1, M(a)) \oplus S_1(M(a), N(a)) \oplus W_3(N(a), P(a)) \oplus W_2(P(a), U_R). \tag{35}$$

See Figure 7.

Observe that this solution coincides with the one in the Construction (B1) if the first stationary wave from U_1 to $M = U_2$ shifts a-component from a_L directly to a_R. The other limit case where the first stationary wave to G_1 is not used gives a connection to the following possibility.

Construction (B3). In this case the Riemann data can be altogether in a

25

arbitrarily small ball in G_2. Assume first that $a_L \geq a_R$. Let

$$U_1 = \mathcal{W}_1(U_L) \cap \mathcal{C}_+, \quad \text{and} \quad U_1^0 \in G_2 + \quad \text{resulted by} \quad W_3(U_1, U_1^o),$$
$$K = \mathcal{W}_1(U_L) \cap \mathcal{C}_-, \quad \text{and} \quad K^0 \in G_2 - \quad \text{resulted by} \quad W_3(K, K^o).$$

(36)

From any state $U \in \mathcal{W}_1(U_L)$, where $\lambda_1(U_L) \leq 0$ (U_L is below U_1 or coincides with U_1), we use a stationary jump to a state U^o, shifting the bottom height from a_L down to a_R. The set of these states U^o form a "composite" curve as

$$\mathcal{W}_1^a(U_L) := \{U^o : \quad \exists W_3(U, U^o) \quad \text{shifting } a_L \quad \text{to } a_R,$$
$$U = (h, u, a_L) \in \mathcal{W}_1(U_L), \lambda_1(U) \leq 0\}. \quad (37)$$

The curve $\mathcal{W}_1^a(U_L)$ is thus a path between U_1^o and K^o. Whenever $\emptyset \neq \mathcal{W}_2^B(U_R) \cap \mathcal{W}_1^a(U_L) = \{U_M^o\}$, a Riemann solution can be determined by

$$W_1(U_L, U_M) \oplus W_3(U_M, U_M^o) \oplus W_2(U_M^o, U_R), \quad (38)$$

where $U_M \in \mathcal{W}_1(U_L)$, provided $U_R \in G_2$ or $\bar{\lambda}_2(U_M^o, U_R) \geq 0$. See Figure 8.

Second, consider the case $a_L < a_R$. Let $\mathcal{C}_+^a$ as in the case for the solution of the type (38). To each $U \in \mathcal{C}_\pm$, a stationary contact to $U^o \in G_2$ downing back $a = a_R$ to $a = a_L$ is possible, since $a_R > a_L$. The set of all these states U^o form two curves denoted by $\mathcal{C}_\pm^a$. Let

$$\{U_1\} = \mathcal{W}_1(U_L) \cap \mathcal{C}_+^a, \quad \text{and} \quad U_1^0 \in \mathcal{C}_+ \quad \text{resulted by} \quad W_3(U_1^o, U_1),$$
$$\{K\} \in \mathcal{W}_1(U_L), \quad \text{and} \quad K^0 \in \mathcal{C}_- \quad \text{resulted by} \quad W_3(K^o, K)$$

(39)

decreasing a_R to a_L. From any state $U \in \mathcal{W}_1(U_L)$, $\lambda_1(U) \leq \lambda_1(U_1)$, there is a stationary jump to a state U^o, shifting the bottom height from a_L to a_R. The set of these states U^o form a composite curve also denoted by $\mathcal{W}_1^a(U_L)$. Whenever $\emptyset \neq \mathcal{W}_2^B(U_R) \cap \mathcal{W}_1^a(U_L) = \{U_M^o\}$, a Riemann solution can be determined by

$$W_1(U_L, U_M) \oplus W_3(U_M, U_M^o) \oplus W_2(U_M^o, U_R), \quad (40)$$

where $U_M \in \mathcal{W}_1(U_L)$, provided $U_R \in G_2$ or $\bar{\lambda}_2(U_M^o, U_R) \geq 0$.

Remark 5. In both cases $a_L > a_R$ and $a_L \leq a_R$, the condition for $\mathcal{W}_2^B(U_R) \cap \mathcal{W}_1^a(U_L) \neq \emptyset$ is that U_1^0 lies above $\mathcal{W}_2^B(U_R)$ and K^o lies below $\mathcal{W}_2^B(U_R)$. See Figure 9.
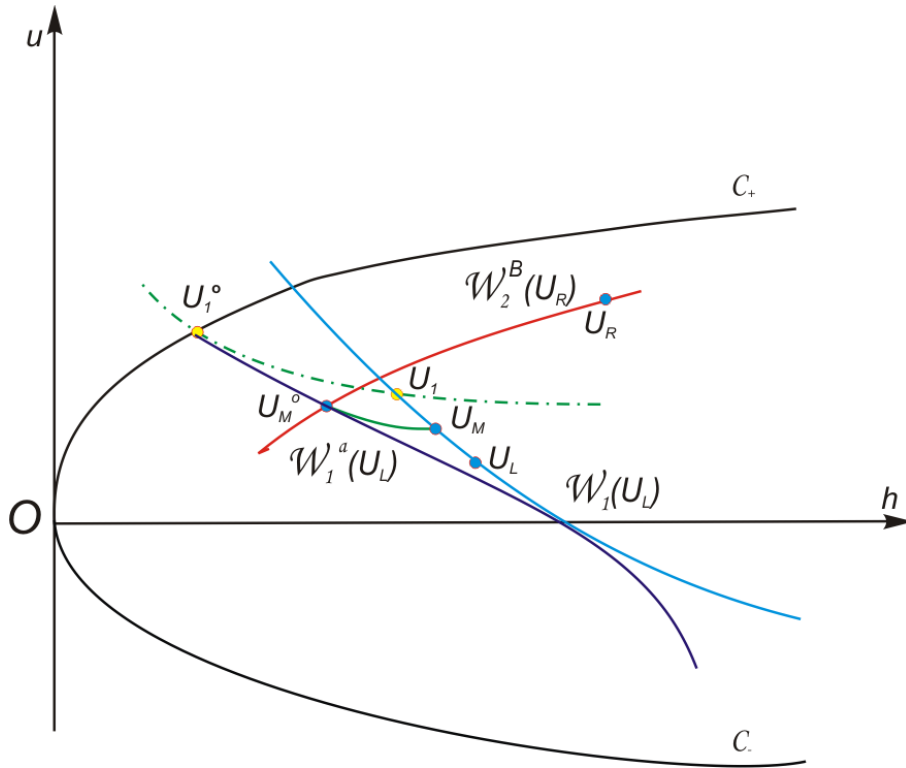
Figure 8: Construction (B3), $a_L > a_R$: A solution of the form (38)

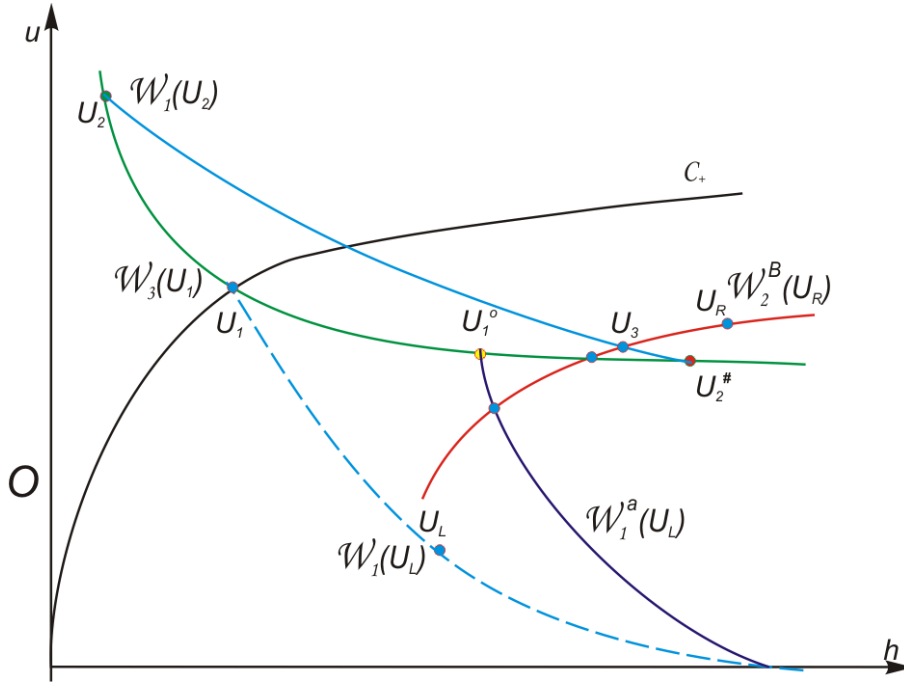Figure 9: Construction (B3), $a_L < a_R$: A solution of the form (40)

Figure 10: Regime (B): Solving the question whether $h_1^o < h_2^\#$ would determine the uniqueness of the Riemann problem or there can be multiple solutions for $U_L \in G_2$ and $a_L > a_R$ (see Theorem 3.3).

Let us now we discuss about the existence and uniqueness. Assume first that $a_L \leq a_R$. In this case, only Constructions (B1) and (B3) are available. The limit case of (31) of (B1) when $U_3 \equiv U_2$ coincides with the limit case of (38) of (B3). Thus, the union $\mathcal{W}_1(U_2) \cup \mathcal{W}_1^a(U_L)$ form a continuous decreasing curve (the curve can be considered as the graph of u being a decreasing function of h) and that $\mathcal{W}_1(U_2)$ and $\mathcal{W}_1^a(U_L)$ meets only at one point U_2. Since $\mathcal{W}_2^B(U_R)$ is an increasing curve, there always a unique intersection point of $\mathcal{W}_2^B(U_R)$ and the union $\mathcal{W}_1(U_2) \cup \mathcal{W}_1^a(U_L)$ if K^o lies below or on the curve $\mathcal{W}_2^B(U_R)$. This implies that the Riemann problem for (1)-(2) always admits a unique solution if K^o lies below or on the curve $\mathcal{W}_2^B(U_R)$.

Next, assume that $a_L > a_R$. Let $U_1^o \in G_2$ denote the state resulted from a stationary wave from $U_1 \in \mathcal{C}_+$. Observe that both U_1^o and $U_2^\#$ belong to $\mathcal{W}_3(U_1)$. Whenever U_1^o lies above $U^\#$ on $\mathcal{W}_3(U_1)$, there are three distinct solutions. Otherwise, there is at most one solution. See Figure 10.

Theorem 3.3 (Riemann problem for shallow water equations). *Given a left-hand state $U_L \in G_2$.*

(a) **Existence.** *The Riemann problem (1)-(3) admits a solution if K^o lies below or on the curve $\mathcal{W}_2^B(U_R)$, and that if $\mathcal{W}_2^B(U_R)$ intersects with $\mathcal{W}_1^a(U_L)$ at some point $U_M^o \in G_1-$, then $\bar{\lambda}_2(U_M^o, U_R) \geq 0$.*

(b) **Regime of uniqueness.** *The Riemann problem (1)-(3) has at most one solution if*

– *either $a_L \leq a_R$;*

– *or $a_L > a_R$, $h_1^o \geq h_2^{\#}$, where U_2 is defined in (31);*

– *or $a_L > a_R$, $h_1^o < h_2^{\#}$, and the states U_1^o and $U_2^{\#}$ are located on the same side with respect to the curve $\mathcal{W}_2^B(U_R)$.*

(c) **Multiple solutions.** *If $a_L > a_R$, $h_1^o < h_2^{\#}$, and U_1^o lies above the curve $\mathcal{W}_2^B(U_R)$ and $U_2^{\#}$ lies below the curve $\mathcal{W}_2^B(U_R)$, then the Riemann problem (1)-(3) has three solutions.*

Example. We provide some numerical experiments computing $h_1^o, h_2^{\#}$ to illustrate the cases of Theorem 3.3 (see Tables B1, B2, and B3). All experiments give the same result: $h_1^o > h_2^{\#}$.

Table B1			
States	U_L	U_1^o	$U_2^{\#}$
Water Height h	3	1.819500899801235	1.768961248574716
Velocity u	0.5	3.032474262659020	3.119112786658156
Bottom Level a	1.1	1.000000000000000	1.000000000000000

Table B2			
States	U_L	U_1^o	$U_2^{\#}$
Water Height h	3	1.707571536932233	1.656818524474798
Velocity u	0.1	2.901359698616083	2.990236508448978
Bottom Level a	1.1	1.000000000000000	1.000000000000000

Table B3			
States	U_L	U_1^o	$U_2^{\#}$
Water Height h	3	3.187878980786353	2.574902018055705
Velocity u	1	1.969891931767155	2.438841182952260
Bottom Level a	2	1.000000000000000	1.000000000000000

Remark 6. We conjecture that $h_1^o > h_2^{\#}$. If this conjecture is verified, then Theorem 3.3 implies that the Riemann problem always has at most one solution for $U_L \in G_2$.

3.3. Continuous dependence of the set of solutions

As seen in the previous subsections, Riemann solutions are constructed based on a given left-hand state U_L. The Riemann problem for (1)-(2) admits up to three solutions for data in certain regions. Therefore, this implies that the initial-value problem for (1)-(2) is ill-posed. However, connectivity between the types of Riemann solutions helps to determine the continuous dependence of the set of solutions on Riemann data. This means that the Haussdoff distance between the sets of all solutions of the Riemann problem depends continuously on the Riemann data. In fact, we first note that for each construction (A) and (B), the structure of solution changes continuously when U_R moves to make the case-to-case change. For example, the Construction (A1) changes continuously to (A2), the case (A2) itself changes continuously to (A3). Similar remarks for the cases (B1), (B2) and (B3), as observed earlier for the continuity of the wave patterns. Thus, the set of solutions depends continuously on the right-hand side U_R for each case $U_L \in G_1 \cup \mathcal{C}_+$ and $U_L \in G_2$. In order to show that the set of solutions depends continuously on Riemann data, we weed only to point out that when U_L moves from G_1 to G_2, the change in structure of solution is continuous. But this is true, since when U_L tends to $\mathcal{C}_+$ on each side, the solution of the Construction (A1) and (B1) approach to each other, and the solution of the Construction (A3) and (B3) approach to each other as long as the solutions make sense. If $a_L \geq a_R$, these types eventually coincide on $\mathcal{C}_+$. Thus, we arrive at the following theorem.

Theorem 3.4 (Continuous dependence)**.** *The set of solutions of the Riemann problem for (1)-(2), whenever it exists, depends continuously on the Riemann data.*

4. A Godunov-type algorithm

4.1. A well-balanced, quasi-conservative scheme

Given a uniform time step Δt, and a spacial mesh size Δx, setting $x_i = i\Delta x, i \in \mathbf{Z}$, and $t^n = n\Delta t, n \in \mathbf{N}$, we denote U_i^n to be an approximation of the exact value $U(x_i, t^n)$. Set

$$U = \begin{pmatrix} h \\ hu \end{pmatrix}, \quad F(U) = \begin{pmatrix} hu \\ h(u^2 + g\frac{h}{2}) \end{pmatrix}, \quad S(U) = \begin{pmatrix} 0 \\ -gh \end{pmatrix} \partial_x a.$$

The system (1)-(2) can be written in the compact form

$$\partial_t U + \partial_x F(U) = S(U)\partial_x a, \quad t > 0, x \in \mathbf{R}, \tag{41}$$

Let us be given the initial condition

$$U(x, 0) = U_0(x), \quad x \in \mathbf{R}, \tag{42}$$

Then, the discrete initial values U_i^0 are given by

$$U_i^0 = \frac{1}{\Delta x} \int_{x_{i-1/2}}^{x_{i+1/2}} U_0(x)dx. \tag{43}$$

Suppose U^n is known and U^n is constant on each interval $(x_{i-1/2}, x_{i+1/2})$ vi $i \in \mathbf{Z}$. On each cell (x_{i-1}, x_i) we determine the exact solution of the Riemann problem for

$$\partial_t U(x, t) + \partial_x F(U(x, t)) = S(U)\partial_x a, \quad \text{on } \mathbf{R} \times (t^n, t^{n+1}], \tag{44}$$

subject to the initial condition

$$U(x, t^n) = \begin{cases} U_{i-1}^n, & x < x_{i-1/2}, \\ U_i^n, & x > x_{i-1/2}. \end{cases} \tag{45}$$

Denote this solution by $U(x, t; U_{i-1}^n, U_i^n)$. Use these solutions of the local Riemann problems we define the function V by

$$V(x, t) := \begin{cases} U(x, t; U_{i-1}^n, U_i^n), & x_{i-1/2} < x \le x_i, t^n \le t \le t^{n+1}, \\ U(x, t; U_i^n, U_{i+1}^n), & x_i < x \le x_{i+1/2}, t^n \le t \le t^{n+1} \end{cases}$$

As for the initial values, we have to ensure that the approximation U_i^{n+1} at time t^{n+1} is constant on $(x_{i-1/2}, x_{i+1/2})$ for all $i \in \mathbf{Z}$. Therefore, we define the new value U_i^{n+1} at the time $t = t^{n+1}$ by

$$U_i^{n+1} = \frac{1}{\Delta x} \int_{x_{i-1/2}}^{x_{i+1/2}} V(x, t^{n+1}) dx. \tag{46}$$

This means U_i^{n+1} is the mean value of V on $(x_{i-1/2}, x_{i+1/2})$ and thus contains parts of $U(x, t; U_{i-1}^n, U_i^n)$ and $U(x, t; U_i^n, U_{i+1}^n)$. To ensure that the solutions of two consecutive local Riemann problems do not coincide, we assume that the CFL condition holds:

$$\frac{\Delta t}{\Delta x} \max |\lambda_i| \leq \frac{1}{2},$$

where λ_i denote the eigenvalues of $DF(U)$.

Suppose now V is an exact solution on $(x_{i-1/2}, x_{i+1/2})$. Since the a-component is constant in $(x_{i-1/2}, x_{i+1/2})$, the right-hand side of (1) vanishes for V. Thus, the standard Godunov scheme is in *quasi-conservative form*:

$$U_i^{n+1} = U_i^n - \frac{\Delta t}{\Delta x} (F(U(x_{i+1/2}-, t^{n+1}; U_i^n, U_{i+1}^n)) - F(U(x_{i-1/2}+, t^{n+1}; U_{i-1}^n, U_i^n))). \tag{47}$$

One might think that in the scheme (47) the source term is incorporated into the local Riemann problem.

The Godunov scheme (47) is capable of capturing exactly equilibria. Therefore (47) is a *well-balanced* scheme. In fact, let us be given the initial data U^0 to be equilibrium states of a stationary wave. Then, on each cell $x_{i-1/2} < x < x_{i+1/2}, t^n < t \leq t^{n+1}$ the exact Riemann solution is constant. Thus, $U(x_{i+1/2}-, t^n; U_i^n, U_{i+1}^n) = U(x_{i-1/2}+, t^n; U_{i-1}^n, U_i^n)$ and so $U_i^{n+1} = U_i^n = U_i^0$ for all $i \in \mathbf{Z}$ and $n \geq 0$. When there are multiple Riemann solutions, any of them can be taken. We note that this is still determinate, as indicated by Theorem 3.2.

4.2. The computations of Riemann solvers

Given any Riemann data (U_L, U_R), denote by $U(x, t; U_L, U_R)$ the Riemann solution corresponding to the Riemann data (U_L, U_R). To build the Godunov scheme (47) we will specify the values $U(0\pm, \Delta t; U_L, U_R)$ for an arbitrary and fixed number $\Delta t > 0$.

Riemann solver (A1). We present a computing strategy for the Riemann solutions (24) as follows.

(i) The state $U_L^o = (h_L^o, u_L^o, a_R)$: $h_L^o = \bar{h}(a_R) = h_1(a_R)$, where $h_1(a_R)$ is the smaller root of the nonlinear equation (16), described by Lemma 3.1, and can be computed using Lemma 2.3. $u_L^o = u_L h_L / h_L^o$.

(ii) The state $U_M = (h_M, u_M, a_R)$ is the intersection point of the wave curves $\mathcal{W}_1(U_L^o)$ and $\mathcal{W}_2^B(U_R)$, see (13). Equating the u-component for these two curves leads to a strictly increasing and strictly convex function in h. Thus, the h-component of the intersection point h_2 can be computed using the Newton's method.

The Riemann solver (A1) relying on Construction (A1) yields

$$\begin{aligned} U(0-, \Delta t; U_L, U_R) &= U_L, \\ U(0+, \Delta t; U_L, U_R) &= U_L^o. \end{aligned} \tag{48}$$

This implies that the Godunov scheme (47) using the Riemann solver 1 becomes

$$U_i^{n+1} = U_i^n - \frac{\Delta t}{\Delta x}(F(U_i^n) - F((U_{i-1}^n)^o)), \tag{49}$$

where U^o defined as in (48).

Riemann solver (A2).

The states of the Riemann solution (26) can be found as follows.

(1) The state $U_M = (h_M, u_M, a_R)$ is determined by

$$\{U_M\} = \mathcal{W}_3(U_L) \cap \mathcal{W}_2^B(U_R).$$

(2) The states $U_1 = (h_1, u_1, a_1), U_2 = (h_2, u_2, a_1)$ are determined by using the corresponding "half-way" shifting in a component from the stationary contact from U_L to U_1 and the stationary contact from U_2 to U_M, and using the fact that $U_2 = U_1^\#$, (see Lemma 3.1):

$$\begin{aligned} a_1 &= a_L + \frac{u_L^2 - u_1^2}{2g} + h_L - h_1 = a_M + \frac{u_M^2 - u_2^2}{2g} + h_M - h_2, \\ u_1 &= \frac{u_L h_L}{h_1}, \\ h_2 &= \frac{-h_1 + \sqrt{h_1^2 + 8h_1 u_1^2 / g}}{2}, \\ u_2 &= \frac{u_M h_M}{h_2}. \end{aligned} \tag{50}$$

34

It is not difficult to check that the system (50) can yield a scalar equation for h_1. The Riemann solver (A2) relying Construction (A2) gives

$$U(0-, \Delta t; U_L, U_R) = U_L,$$
$$U(0+, \Delta t; U_L, U_R) = U_M = U_M(U_L, U_R). \tag{51}$$

This implies that the Godunov scheme (47) using the Riemann solver 2 becomes

$$U_i^{n+1} = U_i^n - \frac{\Delta t}{\Delta x}(F(U_i^n) - F(U_M(U_{i-1}^n, U_i^n))), \tag{52}$$

where $U_M(U_{i-1}^n, U_i^n))$ is defined as in (51), i.e.

$$\{U_M(U_{i-1}^n, U_i^n))\} = \mathcal{W}_3(U_{i-1}^n) \cap \mathcal{W}_2^B(U_i^n).$$

Since U_M plays a key role in this Riemann solver, we sketch a computing algorithm for U_M as follows. First we observe that if U_R lies below the curve $\mathcal{W}_3(U_L)$ in the (h, u)-plane, then U_M is the intersection point of $\mathcal{W}_3(U_L)$ and $\mathcal{S}_2^B(U_R)$. Otherwise, U_M is the intersection point of $\mathcal{W}_3(U_L)$ and $\mathcal{R}_2^B(U_R)$. Thus,

(i) (Arrival by a 2-shock) If $h_R u_R - h_L u_L < 0$ then h_M is the root of the equation

$$G_1(h) := \frac{h_L u_L}{h} - \left(u_R + (h - h_R)\sqrt{\frac{g}{2}\left(\frac{1}{h} + \frac{1}{h_R}\right)}\right) = 0. \tag{53}$$

(ii) (Arrival by a 2-rarefaction wave) Otherwise, h_M is the root of the equation

$$G_2(h) := \frac{h_L u_L}{h} - (u_R + 2\sqrt{g}(\sqrt{h} - \sqrt{h_R})) = 0. \tag{54}$$

It is easy to see that both functions G_1, G_2 defined by (53) and (54) are strictly convex. Moreover, we have

$$G_1'(h) = -\frac{h_L u_L}{h^2} - \sqrt{\frac{g}{2}}\left(\frac{1}{h} + \frac{2}{h_R} + \frac{h_R}{h^2}\right)\left(\frac{1}{2\sqrt{1/h + 1/h_R}}\right) < 0$$
$$G_2'(h) = -\frac{h_L u_L}{h^2} - \sqrt{\frac{g}{h}} < 0$$

for all $h > 0$. Thus, the Newton method can be applied for both equations (53) and (54) with any starting point.

Riemann solver (A3).

Let us consider Construction (A3) and let

$$A = U_L^{\#}, \quad \{B\} = \mathcal{W}_1(U_L) \cap \mathcal{W}_2^B(U_R).$$

It is easy to see that $U_M = (h_M, u_M, a_L)$ lies on $\mathcal{W}_1(U_L)$ between A and B. We propose a procedure similar to the Bisection method to compute the states of the elementary waves of the Riemann solution (28) as follows. We use the equation of $\mathcal{W}_2^B(U_R) : \Phi_2(U; U_R) = 0$, defined by (13), as a test condition: for U above $\mathcal{W}_2^B(U_R)$, $\Phi_2(U; U_R) > 0$ and for U below it, $\Phi_2(U; U_R) < 0$. Using a stationary jump from any state U on the wave pattern of $\mathcal{W}_1(U_L)$ between A and B to a state U^o shifting a from a_L to a_R. Then, we have

$$\Phi_2(A; U_R) \cdot \Phi_2(B; U_R) < 0.$$

Algorithm 1:

Step 1: An estimate for h_M is given by

$$h_M = \frac{h_A + h_B}{2},$$

$U_M = (h_M, u_M, a_L) \in \mathcal{W}_1(U_L)$, so u_M is computed using the equation (9) with $U_0 = U_L$.

Step 2:

(a) If $\Phi_2(A; U_R) \cdot \Phi_2(U_M; U_R) < 0$, then set $B = U_M$ and return to Step 1;

(b) If $\Phi_2(A; U_R) \cdot \Phi_2(U_M; U_R) > 0$, then set $A = U_M$ and return to Step 1;

(c) If $\Phi_2(A; U_R) \cdot \Phi_2(U_M; U_R) = 0$, terminate the computation.

We can still use an alternative algorithm using the value of a-component as a convergence condition, as follows.

Algorithm 2:

Step 1: Let $A = U_L^{\#}$ and B is the intersection point of $\mathcal{W}_1(U_L)$ and $\{u = 0\}$. An estimate for h_M is given by

$$h_M = \frac{h_A + h_B}{2},$$

and u_M is estimated using the equation (9), so an estimate of U_M is $U_M = (h_M, u_M, a_L) \in \mathcal{W}_1(U_L)$. An estimate for U_M^o is given by

$$\{U_M^o\} = \mathcal{W}_3(U_M) \cap \mathcal{W}_2^B(U_R).$$

Determine the change in a-component for the stationary wave between U_M and U_M^o (see (15))

$$a = a_L + \frac{u_M^2 - (u_M^o)^2}{2g} + h_M - h_M^o.$$

Step 2:

(a) If $a - a_R < 0$, then set $h_A = h_M$ and return to Step 1;

(b) If $a - a_R > 0$, then set $h_B = h_M$ and return to Step 1;

(c) If $a - a_R = 0$, stop the computation.

The Riemann solver (A3) relying on Construction (A3) yields

$$\begin{aligned}
U(0-, \Delta t; U_L, U_R) &= U_M = U_M(U_L, U_R), \\
U(0+, \Delta t; U_L, U_R) &= U_M^o = (U_M(U_L, U_R))^o.
\end{aligned} \tag{55}$$

This implies that the Godunov scheme (47) using the Riemann solver 3 becomes

$$U_i^{n+1} = U_i^n - \frac{\Delta t}{\Delta x}(F(U_M(U_i^n, U_{i+1}^n)) - F(U_M^o(U_{i-1}^n, U_i^n))), \tag{56}$$

where $U_M(U_i^n, U_{i+1}^n)$ and $U_M^o(U_{i-1}^n, U_i^n))$ are defined as in (55).
Riemann solver (B1). The Riemann solver (B1) relying on Construction (B1) gives

$$\begin{aligned}
U(0-, \Delta t; U_L, U_R) &= U_1 = \left((\tfrac{u_L}{3\sqrt{g}} + \tfrac{2}{3}\sqrt{h_L})^2, \tfrac{1}{3}u_L + \tfrac{2}{3}\sqrt{gh_L}, a_L \right) := U_{L,+} \in \mathcal{C}_+, \\
U(0+, \Delta t; U_L, U_R) &= U_2 := U_{L,+o} \in G_1,
\end{aligned} \tag{57}$$

If $a_L \geq a_R$, then

$$\begin{aligned}
U_1 &= \left((\tfrac{u_L}{3\sqrt{g}} + \tfrac{2}{3}\sqrt{h_L})^2, \tfrac{1}{3}u_L + \tfrac{2}{3}\sqrt{gh_L}, a_L \right) := U_{L,+} \in \mathcal{C}_+, \\
U_2 &:= U_{L,+o} \in G_1,
\end{aligned}$$

37

where $U_{L,+o} \in G_1$ is the state resulted by a stationary contact from $U_{L,+} \in C_+$. This implies that the Godunov scheme (47) using the Riemann solver (B1) becomes

$$U_i^{n+1} = U_i^n - \frac{\Delta t}{\Delta x}(F(U_{i,+}^n) - F(U_{i-1,+o}^n)). \tag{58}$$

If $a_L < a_R$, then $U_2 \in C_+$. The computing of U_1 and U_2 can be done similarly as in the Riemann solver (A3).

Riemann solver (B2). The Riemann solver (B2) relying Construction (B2) gives

$$\begin{aligned}
U(0-, \Delta t; U_L, U_R) &= U_1 = \left(\left(\tfrac{u_L}{3\sqrt{g}} + \tfrac{2}{3}\sqrt{h_L}\right)^2, \tfrac{1}{3}u_L + \tfrac{2}{3}\sqrt{gh_L}, a_L\right) := U_{L,+} \in C_+, \\
U(0+, \Delta t; U_L, U_R) &= P = P(U_L, U_R) \in \mathcal{W}_2^B(U_R) \cap \mathcal{W}_3(U_{L,+}).
\end{aligned} \tag{59}$$

This implies that the Godunov scheme (47) using the Riemann solver 2 becomes

$$U_i^{n+1} = U_i^n - \frac{\Delta t}{\Delta x}(F(U_{i,+}^n) - F(P(U_{i-1}^n, U_i^n))), \tag{60}$$

where

$$P(U_{i-1}^n, U_i^n)) = \mathcal{W}_2^B(U_i^n) \cap \mathcal{W}_3(U_{i-1,+}^n).$$

Riemann solver (B3). The Riemann solver (B3) relying on Construction (B3) yields

$$\begin{aligned}
U(0-, \Delta t; U_L, U_R) &= U_M = U_M(U_L, U_R), \\
U(0+, \Delta t; U_L, U_R) &= U_M^o = (U_M(U_L, U_R))^o.
\end{aligned} \tag{61}$$

This implies that the Godunov scheme (47) using the Riemann solver 3 becomes

$$U_i^{n+1} = U_i^n - \frac{\Delta t}{\Delta x}(F(U_M(U_i^n, U_{i+1}^n)) - F(U_M^o(U_{i-1}^n, U_i^n))), \tag{62}$$

where $U_M(U_i^n, U_{i+1}^n)$ and $U_M^o(U_{i-1}^n, U_i^n))$ are defined as in (61). It is easy to see that the determinations of the states $U(0-, \Delta t; U_L, U_R)$ and $U(0+, \Delta t; U_L, U_R)$ by Solvers (A3) and (B3) are the same.

The computing strategies for Solvers (B1), (B2), and (B3) are similar to those of Solvers (A1), (A2), and (A3).

4.3. Building Godunov scheme algorithm

Which Riemann solvers are taken in the Godunov scheme? As seen earlier, in the regions where there are possibly multiple solutions one can take any Riemann solution. Thus, there can be multiple choices to select a Riemann solvers whenever there are several ones. And thus, there can be three extreme cases by preferring one particular Riemann solver whenever it is availbalbe. For example, if we prefer the solutions that has the stationary contact wave in the same region as the left-hand state, then the solvers (A1) and (B3) are selected. This selection gives an algorithm for building the Godunov scheme described as follows.

Building Godunov Scheme Algorithm preferring solvers (A1) and (B3). Let $U_L = U_i^n$ and $U_R = U_{i+1}^n$.

    If $\lambda_1(U_L) \leq 0$
       If $\Phi_2(U_L^{o\#}; U_R) < 0$
         Use Solver (A1)
       elseif $\Phi_2(U_L^{\#o}; U_R) < 0$
         Use Solver (A2)
       else
         Use Solver (A3)
       end
    else
       If $\Phi_2(U_1^o; U_R) > 0$
         Use Solver (B3)
       elseif $\Phi_2(U_2^\#; U_R) > 0$
         Use Solver (B2)
       else
         Use Solver (B1)
       end
    end

5. Numerical experiments (I)

We will demonstrate the efficiency of our Riemann solver in the Godunov method by several numerical tests. For each test we measure the errors between the exact Riemann solution and the approximate solution by the Godunov scheme (47) for $x \in [-1, 1]$ with different mesh sizes of $500, 1000, 2000$

points. In this section as well as in the next section, we take the time $t = 0.1$, the stability condition

$$C.F.L = 0.75$$

and the algorithm for selecting Riemann solvers as described at the end of the last section, unless other information is given.

5.1. Test 1

This test indicates that the Godunov method is capable of maintaining equilibrium states. Let

$$U_0(x) = \begin{cases} U_L = (h_L, u_L, a_L), & x < 0 \\ U_R = (h_R, u_R, a_R), & x > 0, \end{cases} \tag{63}$$

where $U_L = (1, 4, 1.1)$ and $U_R = (0.893267776689718, 4.477940550842711, 1)$. It is not difficult to check that the Riemann problem for (1) with Riemann data (63) admits a stationary contact between these equilibrium states:

$$U(x, t) = U_0(x), \quad x \in \boldsymbol{R}, t > 0. \tag{64}$$

The Figure 11 shows that the stationary contact is well captured by Godunov method using our exact Riemann solver for $x \in [-1, 1]$ with the mesh sizes of 500 points and at the time $t = 0.1$.

5.2. Test 2

In this test, we will approximate a non-stationary Riemann solution with Riemann data $U_L, U_R \in G_1$. Precisely, we consider the Riemann problem for (1)-(2) with the Riemann data

$$U_0(x) = \begin{cases} U_L = (h_L, u_L, a_L) = (0.3, 2, 1.1) \in G_1, & x < 0, \\ U_R = (h_R, u_R, a_R) = (0.4, 2.2, 1) \in G_1, & x > 0. \end{cases} \tag{65}$$
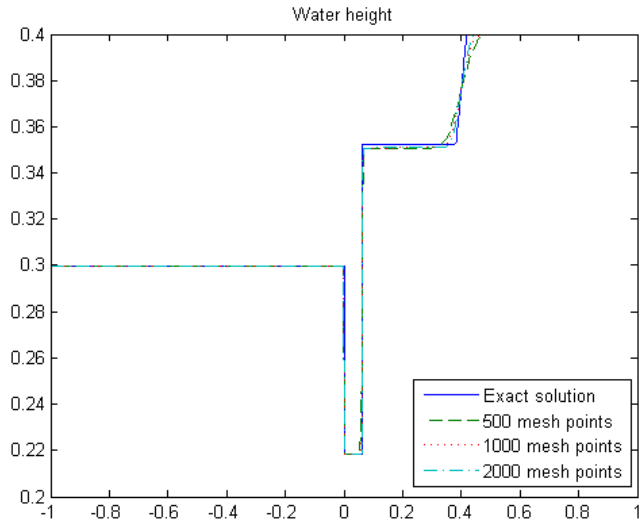
The Riemann problem (1)-(2) with the initial data (65) admits the solution described by Construction 1, where

$$U_1 = (0.21815897, 2.750288, 1)$$
$$U_2 = (0.35252714, 1.9572394, 1).$$
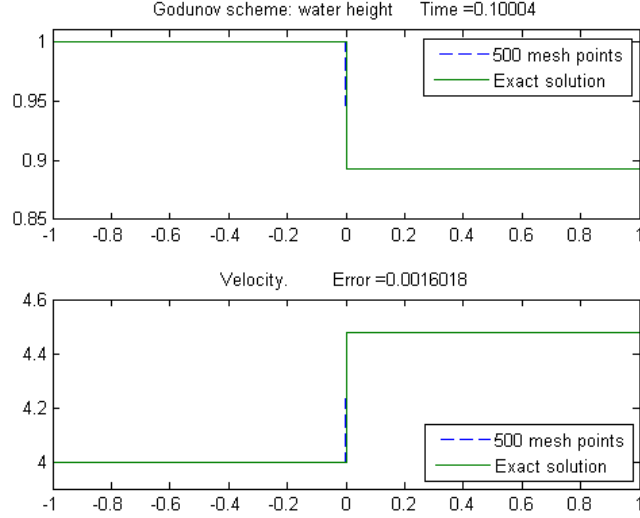
Figure 11: Test 1: A stationary contact wave is captured exactly by Godunov method using our exact Riemann solver

The errors for Test 2 are reported in the Table 66.

$$
\begin{array}{|c|c|}
\hline
N & ||U_h^C - U||_{L^1} \\
\hline
500 & 0.012644 \\
1000 & 0.0087928 \\
2000 & 0.0063773 \\
\hline
\end{array}
\tag{66}
$$

Figures 12, 13 and Table (66) show that approximate solutions are closer to the exact solution when the mesh-size gets smaller.

5.3. Test 3

In this test, we will approximate a non-stationary Riemann solution with Riemann data $U_L, U_R \in G_2$. Precisely, we consider the Riemann problem for (1)-(2) with the Riemann data

$$
U_0(x) = \left\{
\begin{array}{ll}
U_L = (h_L, u_L, a_L) = (2, 0.1, 1.1) \in G_2, & x < 0, \\
U_R = (h_R, u_R, a_R) = (3, 0.12, 1) \in G_2, & x > 0.
\end{array}
\right.
\tag{67}
$$

41

Figure 12: Test 2: Approximations for the water height with different mesh sizes
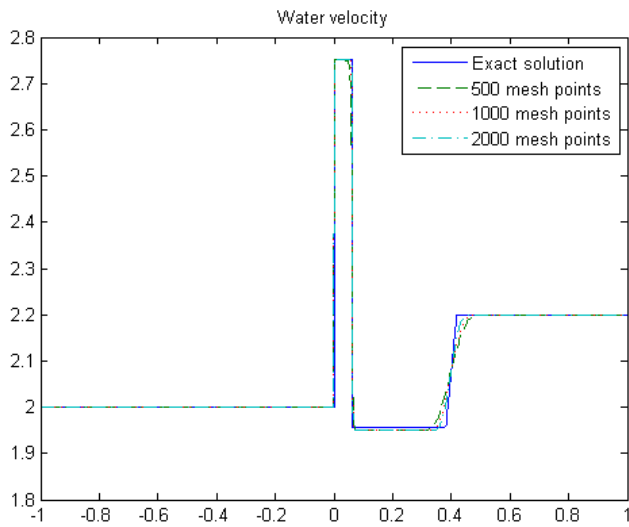
Figure 13: Test 2: Approximations for the water velocity with different mesh sizes

42
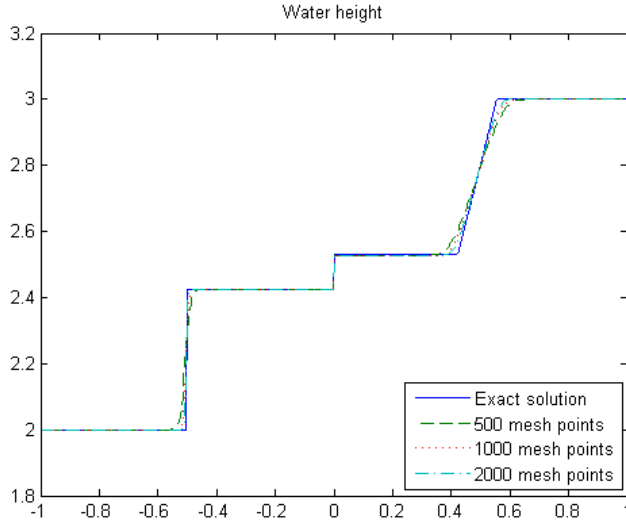
Figure 14: Test 3: Approximations for the water height with different mesh sizes

The Riemann problem (1)-(2) with the initial data (65) admits the solution described by Construction 7, where

$$U_4 = (2.42606, -0.80076542, 1.1)$$
$$U_5 = (2.528661, -0.76827417, 1).$$

The errors for Test 3 are reported in the Table 68.

$$
\begin{array}{c|c}
N & ||U_h^{\mathrm{C}} - U||_{L^1} \\
\hline
500 & 0.041287 \\
1000 & 0.023896 \\
2000 & 0.014076 \\
\end{array}
\tag{68}
$$

Figures 14, 15 and Table 68 show that approximate solutions are closer to the exact solution when the mesh-size gets smaller.

The above tests show the convergence of approximate solutions to the exact solution.

6. Numerical experiments (II). The resonance regime

In the following, we will consider the cases where the Riemann data on the different sides with respect to $\mathcal{C}_+$:

43
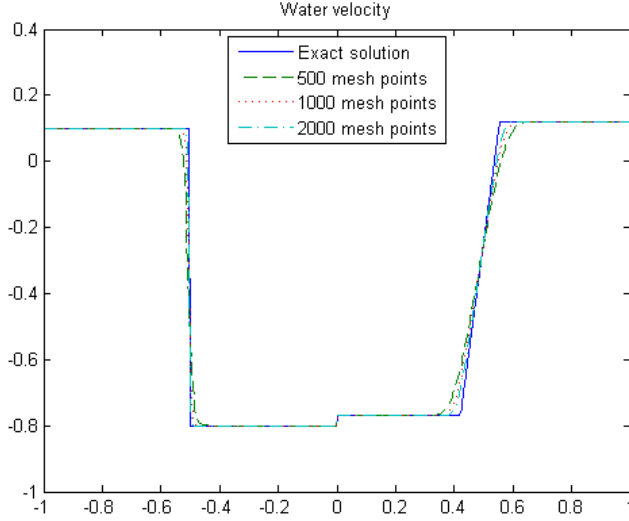
Figure 15: Test 3: Approximations for the water velocity with different mesh sizes

(i) $U_L \in G_1$ and $U_R \in G_2$;

(ii) $U_L \in G_2$ and $U_R \in G_1$.

The solution is evaluated for $x \in [-1, 1]$ with the mesh size of 500 points and at the time $t = 0.1$. We take also

$$C.F.L = 0.75.$$

6.1. Test 4

In this test, $a_L > a_R$, and there is a unique solution. We consider the Riemann problem for (1)-(2) with the Riemann data

$$U_0(x) = \begin{cases} U_L = (h_L, u_L, a_L) = (1, 3, 1.1) \in G_1, & x < 0, \\ U_R = (h_R, u_R, a_R) = (1.2, 0.1, 1) \in G_2, & x > 0. \end{cases} \tag{69}$$

We have

$$h_L^{o\#} = 1.042865405801653 < h_L^{\#o} = 1.213385283426733.$$
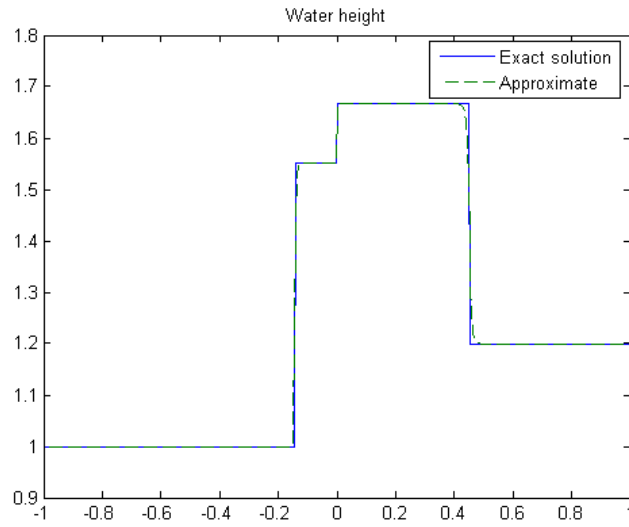
Figure 16: Test 4: (Resonance case) Approximation of water height of the solution (28)
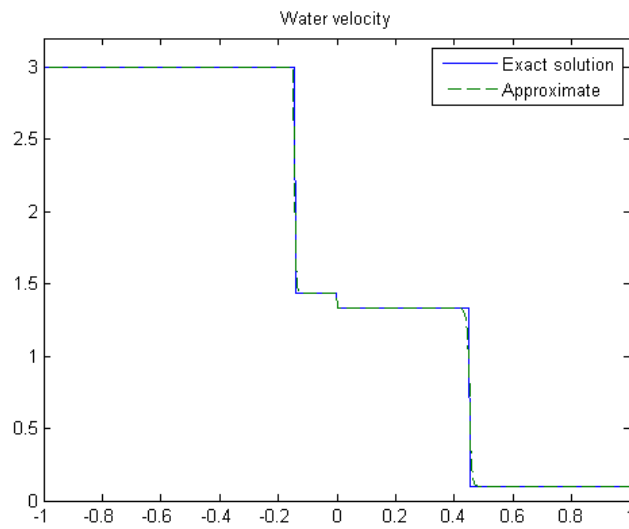
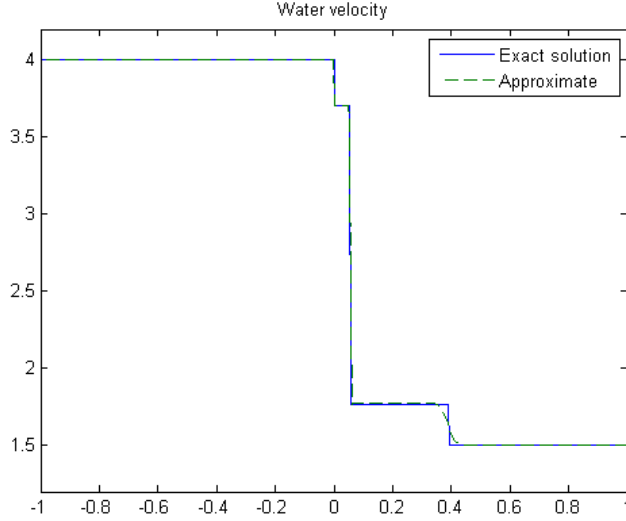Figure 17: Test 4: (Resonance case) Approximation of water velocity of the solution (28)

45
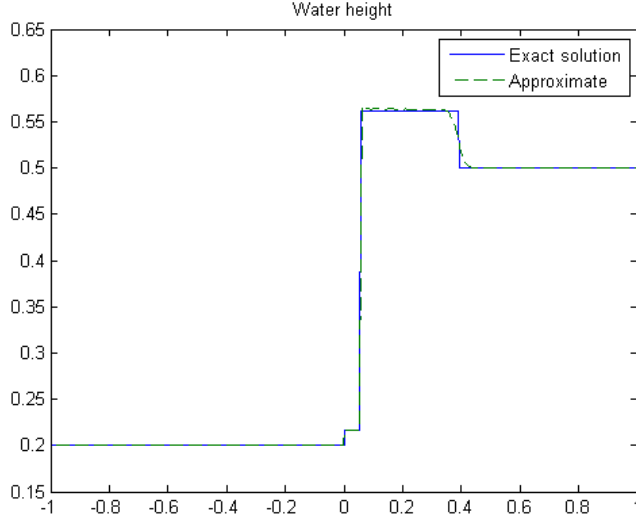
Figure 18: Test 5: (Resonance case) Approximation of water height of the solution (24)

Thus, the Riemann problem for (1)-(2), (69) admits a unique solution of the form (24), according to Theorem (3.2), where

$$U_M = (1.5521168, 1.4328264, 1.1), \quad U_M^o = (1.665941, 1.3349296, 1). \quad (70)$$

The Figures 16-17 show that the Godunov scheme gives good approximate solutions to the exact solution in this resonance case.

6.2. Test 5

In this test, $a_L < a_R$, and there is a unique solution. We consider the Riemann problem for (1)-(2) with the Riemann data

$$U_0(x) = \begin{cases} U_L = (h_L, u_L, a_L) = (0.2, 4, 1) \in G_1, & x < 0, \\ U_R = (h_R, u_R, a_R) = (0.5, 1.5, 1.1) \in G_2, & x > 0. \end{cases} \quad (71)$$

We have

$$U_L^{o\#} = (0.677264819960833, 1.181221844722815),$$
$$\Phi_2(U_L^{o\#}; U_R) = -1.050411375011095 < 0,$$
$$U_L^{\#o} = (0.581828763814630, 1.374974992221044),$$
$$\Phi_2(U_L^{\#o}; U_R) = -0.474326705580410 < 0.$$

46

Figure 19: Test 5: (Resonance case) Approximation of water velocity of the solution (24)

Thus, the Riemann problem for (1)-(2), (69) admits a unique solution of the form (24), according to Theorem (3.2), where

$$U_L^o = (0.21591647, 3.7051366, 1.1), \quad U_M = (0.56185289, 1.7661913, 1.1).$$
$$(72)$$

The Figures 18-19 show that the Godunov scheme gives good approximate solutions to the exact solution in this resonance case.

6.3. Test 6

Next, we provide a test for the case there are multiple solutions. So we consider the Riemann problem for (1)-(2) with the Riemann data

$$U_0(x) = \begin{cases} U_L = (h_L, u_L, a_L) = (0.2, 5, 1) \in G_1, & x < 0, \\ U_R = (h_R, u_R, a_R) = (0.75904946, 1.3410741, 1.2) \in G_2, & x > 0. \end{cases}$$
$$(73)$$

The Riemann problem (1)-(2) with the initial data (73) admits three distinct solutions: one solution of the form (24) with

$$U_L^o = (0.21984063, 4.5487497, 1.2), \quad U_M = (0.7964266, 1.4737915, 1.2) \quad (74)$$
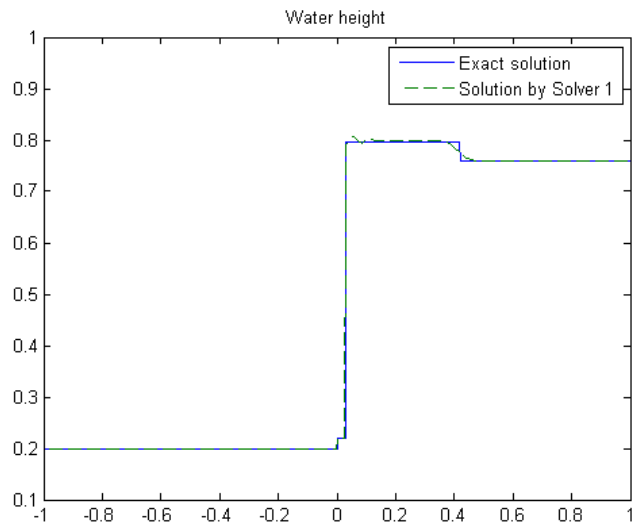
47

Figure 20: Test 6: (Resonance case-Multiple solutions) Approximation of water height of the solution (24) preferred Solver (A1)
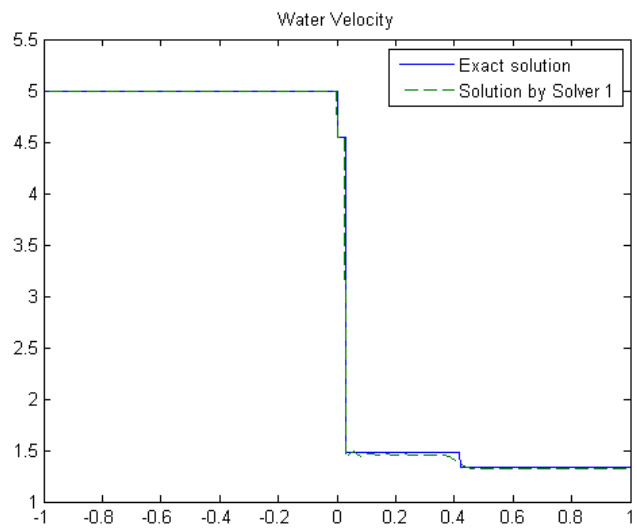

Figure 21: Test 6: (Resonance case-Multiple solutions) Approximation of water velocity of the solution (24) preferred Solver (A1)
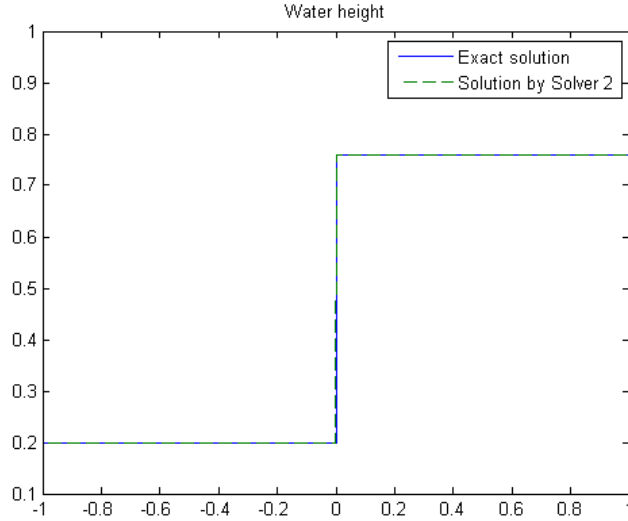
48

Figure 22: Test 6: (Resonance case-Multiple solutions) Approximation of water height of the solution (26) preferred Solver (A2)

one solution of the form (26) with

$$U_M = (0.75904946, 1.3174372, 1.2) \tag{75}$$

which can be seen to be a stationary solution, and one solution of the form (28) with

$$U_M = (0.95328169, 0.89892673, 1), \quad U_M^o = (0.72279573, 1.1855776, 1.2). \tag{76}$$

We could have three extreme choices of a Riemann solver for the Godunov method in this case. This can be seen easily by saying that we prefer a particular Riemann solver whenever it is available.

We can see from Figures 20-21 that if the Solver (A1) is preferred whenever it is available, then the approximate solution approaches the exact solution. The same observation for Solver (A2), see 22-23. However, it is not the case for the Solver (A3): approximate solutions do not converge to the exact Riemann solution by (28), see Figures 24-25.
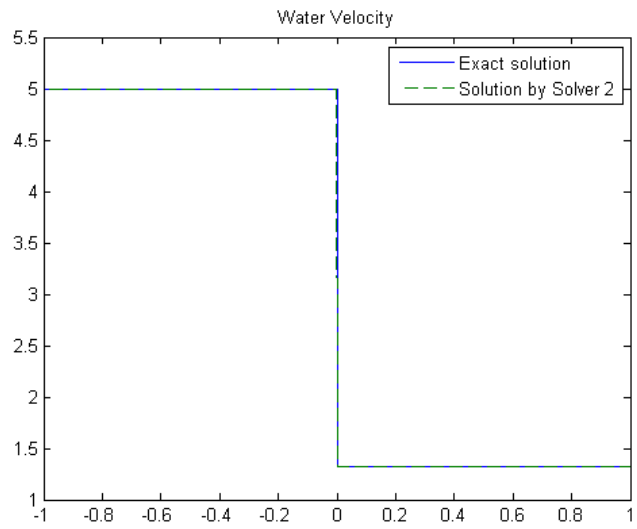
Figure 23: Test 6: (Resonance case-Multiple solutions) Approximation of water velocity of the solution (26) preferred Solver (A2)
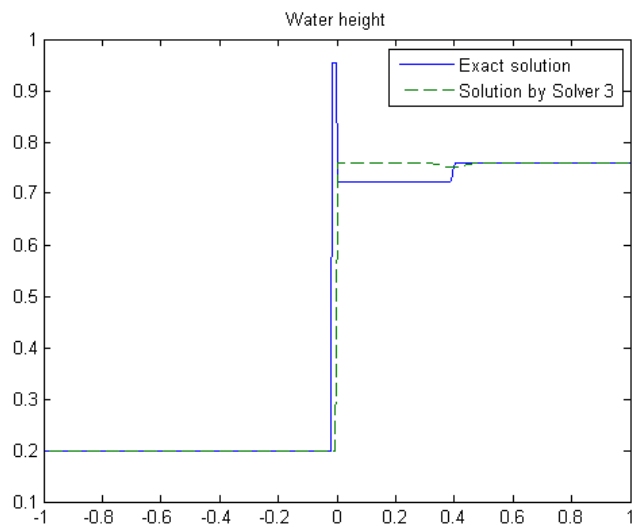

Figure 24: Test 6: (Resonance case-Multiple solutions) Approximation of water height of the solution (28) preferred Solver (A3)
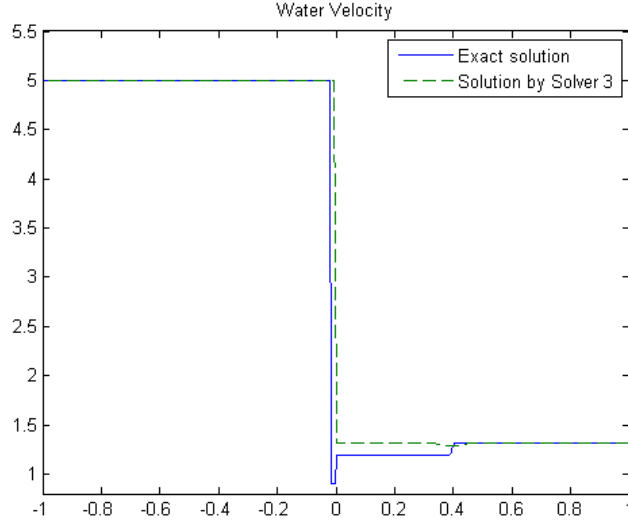
50

Figure 25: Test 6: (Resonance case-Multiple solutions) Approximation of water height of the solution (28) preferred Solver (A3)

6.4. Test 7

We consider the Riemann problem for (1)-(2) with the Riemann data

$$U_0(x) = \begin{cases} U_L = (h_L, u_L, a_L) = (1, 2, 1.1) \in G_2, & x < 0 \in G_1, \\ U_R = (h_R, u_R, a_R) = (0.8, 4, 1) \in G_1, & x > 0. \end{cases} \quad (77)$$

We have

$$h_2^\# = 0.998204556070240 < h_1^o = 1.050890579855180,$$

where $h_2^\#, h_1^o$ are defined as in Theorem (3.3). Thus, the Riemann problem for (1)-(2), (69) admits a unique solution of the form (32), according to Theorem (3.3), where

$$U_1 = (0.77374106, 2.7536634, 1.1), U_2 = (0.58589019, 3.636556, 1), \\ U_3 = (0.6204785, 3.3318107, 1). \quad (78)$$

The Figures 26-27 show that the Godunov scheme generates approximate solutions which do not approach the exact solution in this resonance case.
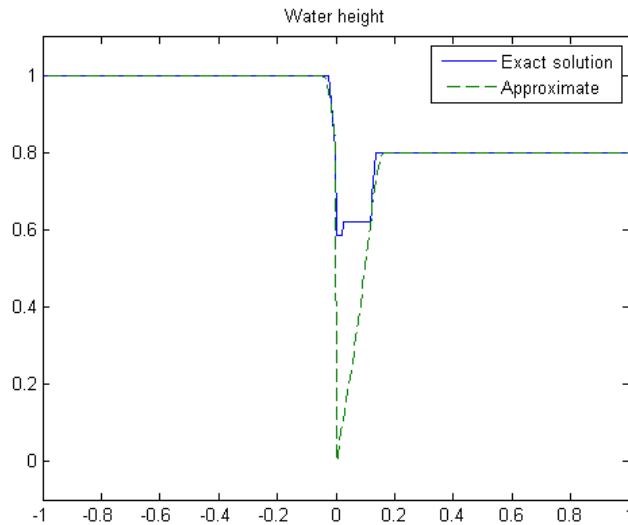
51

Figure 26: Test 7: (Resonance case) Approximation of water height of the solution (32). Godunov scheme generates approximate solutions which do not approach the exact solution in this resonance case.

7. Conclusions and Discussions

We provide above a full description of the Riemann problem for shallow water equations. First, we establish for the first time the existence domain, the uniqueness, as well as the case where there are multiple solutions. Second, we provide the computing strategy for all the Riemann solutions. This particularly gives the rise to define the Godunov scheme for (1). The Godunov scheme, as seen in Section 5, converges in strictly hyperbolic domains. When data belong to both sides of the resonance curve, some tests give convergence, and other tests give divergence. Furthermore, if the Godunov scheme takes the states on the resonance curve give unsatisfactory results.

References

[1] A. Ambroso, C. Chalons, F. Coquel, and T. Galié, Relaxation and numerical approximation of a two-fluid two-pressure diphasic model, *ESAIM: M2AN*, 43:1063-1097, 2009.
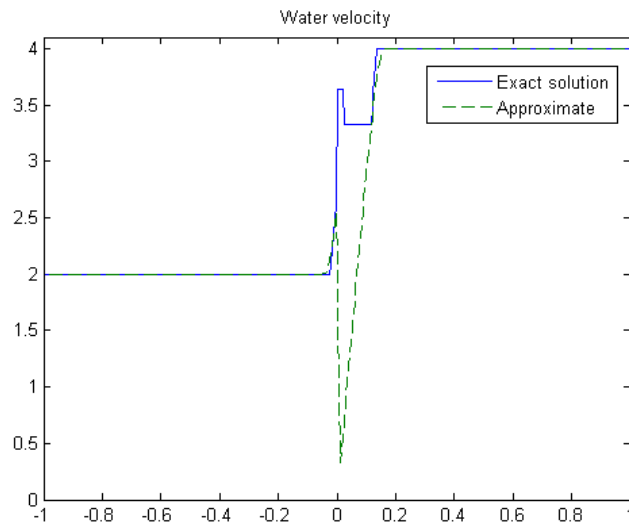
Figure 27: Test 7: (Resonance case) Approximation of water velocity of the solution (32). Godunov scheme generates approximate solutions which do not approach the exact solution in this resonance case.

[2] N. Andrianov and G. Warnecke, On the solution to the Riemann problem for the compressible duct flow, *SIAM J. Appl. Math.*, 64(3):878–901, 2004.

[3] N. Andrianov and G. Warnecke, The Riemann problem for the Baer-Nunziato model of two-phase flows, *J. Comput. Phys.*, 195:434–464, 2004.

[4] E. Audusse, F. Bouchut, M-O. Bristeau, R. Klein, and B. Perthame, A fast and stable well-balanced scheme with hydrostatic reconstruction for shallow water flows, *SIAM J. Sci. Comput.*, 25(6):2050–2065, 2004.

[5] R. Botchorishvili, B. Perthame, and A. Vasseur, Equilibrium schemes for scalar conservation laws with stiff sources, *Math. Comput.*, 72:131–157, 2003.

[6] R. Botchorishvili and O. Pironneau, Finite volume schemes with equilibrium type discretization of source terms for scalar conservation laws, *J. Comput. Phys.*, 187:391–427, 2003.

[7] F. Bouchut, *Nonlinear stability of finite volume methods for hyperbolic*

conservation laws, and well-balanced schemes for sources, Frontiers in Mathematics series, Birkhäuser, 2004.

[8] M.J. Castro, P.G. LeFloch, M.L. Munoz-Ruiz, and C. Pares, Why many theories of shock waves are necessary. Convergence error in formally path-consistent schemes, *J. Comput. Phys.* 227 (2008), 8107–8129.

[9] A. Chinnayya, A.-Y. LeRoux, and N. Seguin, A well-balanced numerical scheme for the approximation of the shallow water equations with topography: the resonance phenomenon, *Int. J. Finite Vol.*, 1(4), 2004.

[10] G. Dal Maso, P.G. LeFloch, and F. Murat, Definition and weak stability of nonconservative products, J. Math. Pures Appl. 74 (1995), 483–548.

[11] T. Gallouët, J.-M. Hérard, and N. Seguin, Numerical modeling of two-phase flows using the two-fluid two-pressure approach, *Math. Models Methods Appl. Sci.*, 14(5):663–700, 2004.

[12] P. Goatin and P.G. LeFloch, The Riemann problem for a class of resonant nonlinear systems of balance laws, *Ann. Inst. H. Poincar Anal. NonLinéaire*, 21:881–902, 2004.

[13] L. Gosse, A well-balanced flux-vector splitting scheme designed for hyperbolic systems of conservation laws with source terms, *Comput. Math. Appl.*, 39:135–159, 2000.

[14] J.M. Greenberg and A.Y. Leroux, A well-balanced scheme for the numerical processing of source terms in hyperbolic equations, *SIAM J. Numer. Anal.*, 33:1–16, 1996.

[15] J.M. Greenberg, A.Y. Leroux, R. Baraille, and A. Noussair, Analysis and approximation of conservation laws with source terms, *SIAM J. Numer. Anal.*, 34:1980–2007, 1997.

[16] T.Y. Hou and P.G. LeFloch, Why nonconservative schemes converge to wrong solutions. Error analysis, Math. of Comput. 62 (1994), 497–530.

[17] E. Isaacson and B. Temple, Nonlinear resonance in systems of conservation laws, *SIAM J. Appl. Math.*, 52:1260–1278, 1992.

[18] E. Isaacson and B. Temple, Convergence of the 2×2 godunov method for a general resonant nonlinear balance law, *SIAM J. Appl. Math.*, 55:625–640, 1995.

[19] S. Jin and X. Wen, An efficient method for computing hyperbolic systems with gometrical source terms having concentrations, *J. Comput. Math.*, 22:230–249, 2004.

[20] S. Jin and X. Wen, Two interface type numerical methods for computing hyperbolic systems with gometrical source terms having concentrations, *SIAM J. Sci. Comput.*, 26:2079–2101, 2005.

[21] D. Kröner, P.G. LeFloch, and M.D. Thanh, The minimum entropy principle for fluid flows in a nozzle with discntinuous crosssection, *ESAIM: M2AN*, 42:425–442, 2008.

[22] D. Kröner and M.D. Thanh, Numerical solutions to compressible flows in a nozzle with variable cross-section, *SIAM J. Numer. Anal.*, 43(2):796–824, 2005.

[23] M-H. Lallemand and R. Saurel, Pressure relaxation procedures for multiphase compressible flows, *INRIA Report, No. 4038*, 2000.

[24] P.G. LeFloch, Entropy weak solutions to nonlinear hyperbolic systems in nonconservative form, Comm. Part. Diff. Equa. 13 (1988), 669–727.

[25] P.G. LeFloch, Shock waves for nonlinear hyperbolic systems in nonconservative form, Institute for Math. and its Appl., Minneapolis, Preprint# 593, 1989 (unpublished).

[26] P.G. LeFloch and T.-P. Liu, Existence theory for nonlinear hyperbolic systems in nonconservative form, Forum Math. 5 (1993), 261–280.

[27] P.G. LeFloch and M. Mohamadian, Why many shock wave theories are necessary. Fourth-order models, kinetic functions, and equivalent equations, J. Comput. Phys. 227 (2008), 4162–4189.

[28] P.G. LeFloch and M.D. Thanh, The Riemann problem for fluid flows in a nozzle with discontinuous cross-section, *Comm. Math. Sci.*, 1(4):763–797, 2003.

[29] P.G. LeFloch and M.D. Thanh, The Riemann problem for shallow water equations with discontinuous topography, *Comm. Math. Sci.*, 5(4):865–885, 2007.

[30] D. Marchesin and P.J. Paes-Leme, A Riemann problem in gas dynamics with bifurcation. Hyperbolic partial differential equations III, *Comput. Math. Appl. (Part A)*, 12:433–455, 1986.

[31] Md. Fazlul K. M.D. Thanh and A. Izani Md. Ismail, Well-balanced scheme for shallow water equations with arbitrary topography, *Inter. J. Dyn. Sys. and Diff. Eqs.*, 1:196–204, 2008.

[32] R. Saurel and R. Abgrall, A multi-phase godunov method for compressible multifluid and multiphase flows, *J. Comput. Phys.*, 150:425–467, 1999.

[33] M.D. Thanh, The Riemann problem for a non-isentropic fluid in a nozzle with discontinuous cross-sectional area, *SIAM J. Appl. Math.*, 69(6):1501–1519, 2009.

[34] M.D. Thanh and A. Izani Md. Ismail, Well-balanced scheme for a one-pressure model of two-phase flows, *Phys. Scr.*, 79:065401, 2009.